Received January 1998
Accepted March 1998

A finite volume scheme for two-dimensional chemically reactive hypersonic flow

Enrico Bertolazzi
Dipartimento di Ingegneria Meccanica e Strutturale, Laboratorio di Matematica Applicata e Meccanica Computazionale, Facoltà di Ingegneria, Università degli Studi di Trento, Mesiano, Trento, Italy

Introduction

The behaviour of inviscid flow at hypersonic regimes is characterised by strong shocks, very high temperatures and chemical reactions whose relaxation times are much smaller than the typical time scales of transport phenomena. These complex physical processes are strongly coupled to each other, thus making a difficult task the numerical solution of Euler equations for the hypersonic flow of a mixture of chemically reactive specie. In order to obtain shock capturing methods and to avoid non-physical solutions, conservative schemes must be used. Also physical constraints, such as non-negativity of densities and energies, must be respected. Furthermore, the nonlinear chemistry terms lead to severe time-step limitations for the time explicit schemes, well beyond the CFL stability restriction. Therefore, some kinds of implicit in time discretization have been used (see Häuser *et al.,* 1989; Schröder and Hartman, 1992; Toon and Kwak, 1992). A semi-implicit, finite volume scheme, is here proposed, which solves the two-dimensional Euler equations for a mixture of chemically reactive specie on general, unstructured grids. The specie here considered are N_2, O_2, NO, N and O. Three vibrational energies are taken into account for the diatomic specie.

The time step advancing procedure is based on a semi-implicit discretization in order to have good stability properties typical of implicit scheme and low computational costs typical of explicit schemes. The time discretization of the highly non-linear terms is implicit. The advective terms are discretized by a semi-implicit upwind method based on a flux vector splitting. This discretization procedure results in a set of weakly nonlinear, partially decoupled equations. Specifically, the discrete mass conservation equations are fully decoupled from all the other equations, the discrete equations for the vibrational energies are decoupled from the momentum and total energy equation, finally the momentum and energy equations are mutually decoupled. The solution algorithm is described as follows. First, the set of equations involving the non-linear reaction terms are solved by an iterative method. Once the specie densities have been determined, the vibrational energies are computed by solving three linear systems, whose matrices are M-matrices. Finally,

International Journal of Numerical Methods for Heat & Fluid Flow
Vol. 8 No. 8, 1998, pp. 888-933.

momentum and the total energy are computed by solving three linear systems, whose matrices are M-matrices. We prove the existence of a discretized solution of the full nonlinear system for any time step. The present scheme is fully conservative and ensures non-negativity of the densities and vibrational energies for arbitrarily large time steps.

The equations

The two dimensional Euler equations with chemically reactive terms are written in integral form as:

$$\frac{\partial}{\partial t}\iint_{\mathcal{S}} \rho_k \, d\mathcal{S} + \oint_{\partial\mathcal{S}} \rho_k \mathbf{v}\cdot\mathbf{n}\, d\ell = \iint_{\mathcal{S}} W_k \, d\mathcal{S}, \tag{1a}$$

$$\frac{\partial}{\partial t}\iint_{\mathcal{S}} \mathcal{E}_{\mathrm{v}_j} \, d\mathcal{S} + \oint_{\partial\mathcal{S}} \mathcal{E}_{\mathrm{v}_j}\mathbf{v}\cdot\mathbf{n}\, d\ell = \iint_{\mathcal{S}} \frac{\mathcal{E}_{\mathrm{eq}_j} - \mathcal{E}_{\mathrm{v}_j}}{\tau_j} \, d\mathcal{S} + \iint_{\mathcal{S}} \frac{W_j^+ \mathcal{E}_{\mathrm{eq}_j} + W_j^- \mathcal{E}_{\mathrm{v}_j}}{\rho_j} \, d\mathcal{S}, \tag{1b}$$

$$\frac{\partial}{\partial t}\iint_{\mathcal{S}} m_x \, d\mathcal{S} + \oint_{\partial\mathcal{S}} m_x \mathbf{v}\cdot\mathbf{n} + p n_x \, d\ell = 0, \tag{1c}$$

$$\frac{\partial}{\partial t}\iint_{\mathcal{S}} m_y \, d\mathcal{S} + \oint_{\partial\mathcal{S}} m_y \mathbf{v}\cdot\mathbf{n} + p n_y \, d\ell = 0, \tag{1d}$$

$$\frac{\partial}{\partial t}\iint_{\mathcal{S}} E \, d\mathcal{S} + \oint_{\partial\mathcal{S}} (E + p)\,\mathbf{v}\cdot\mathbf{n}\, d\ell = 0, \tag{1e}$$

with $k = 1, \ldots, 5$ and $j = 1, 2, 3$; $\mathcal{S}$ is the 2D integration volume and $\partial\mathcal{S}$ denotes its boundary. The vector $\mathbf{n} = [n_x, n_y]^T$ denotes the outer normal. The vector $\mathbf{v} = [v_x, v_y]^T$ denotes velocity and $\mathbf{v}\cdot\mathbf{n}$ denotes the outer normal velocity component.

Equation (1a) represents the conservation of the mass densities where ρ_1, ρ_2, ρ_3, ρ_4 and ρ_5 are the mass densities of the specie N_2, O_2, NO, N and O, respectively. The total mass density is denoted by $\rho = \rho_1 + \rho_2 + \rho_3 + \rho_4 + \rho_5$. Each source term W_k models the chemical reactions involving the kth specie.

Equation (1b) represents the conservation of the vibrational energies, $\mathcal{E}_{\mathrm{v}1}$, $\mathcal{E}_{\mathrm{v}2}$ and $\mathcal{E}_{\mathrm{v}3}$ associated with the diatomic specie N_2, O_2 and NO, respectively. The vibrational energies $\mathcal{E}_{\mathrm{v}j}$ are correlated to the vibrational temperatures T_{vj} and the equilibrium energies $\mathcal{E}\mathrm{eq}_j$ are correlated to the translational temperature T as follows:

$$\mathcal{E}_{\mathrm{eq}_j} = \frac{\rho_j \theta_j \mathcal{R}}{\mathcal{M}_j \left(\exp\left(\frac{\theta_j}{T}\right) - 1\right)}, \quad \mathcal{E}_{\mathrm{v}_j} = \frac{\rho_j \theta_j \mathcal{R}}{\mathcal{M}_j \left(\exp\left(\frac{\theta_j}{T_{vj}}\right) - 1\right)},$$

with $j = 1, 2, 3$. The constants θ_j are the characteristic vibrational temperatures obtained via spectroscopic measurements. They are taken to be $\theta_1 = 3395K$, $\theta_2 = 2239K$ and $\theta_3 = 2817K$ (Candler, 1988). The Landau-Teller relaxation time τ_j in equation (1b) are given by

$$\tau_j = \frac{\sum_{k=1}^{5} \frac{\rho_k}{\mathcal{M}_k} \exp\left(A_j\left(T^{-\frac{1}{3}} - 0,015\,\mu_{i,j}^{\frac{1}{4}}\right) - 18,42\right)}{\frac{p}{101325}\sum_{k=1}^{5}\frac{\rho_k}{\mathcal{M}_k}}, \qquad \mu_{j,k} = 1000\frac{\mathcal{M}_j\mathcal{M}_k}{\mathcal{M}_j + \mathcal{M}_k}$$

where

$$A_1 = 220, \qquad A_2 = 129, \qquad A_3 = 168$$

and $\mathcal{M}_1$, $\mathcal{M}_2$, $\mathcal{M}_3$, $\mathcal{M}_4$, $\mathcal{M}_5$ are the molecular weights of the chemical specie N_2, O_2, NO, N and O respectively. The unit of pressure, temperature, and molecular mass are Pascal, Kelvin and *kg/mole*. These semi-empirical relations are known to be valid over a temperature range from 300K to 9000K (Candler, 1988; Häuser *et al.*, 1989; Millikan and White, 1963).

Equations (1c)-(1d) express the linear momenta conservation, whose components, in the x and y directions, are $m_x = \rho v_x$ and $m_y = \rho v_y$, respectively.

Equation (1e) expresses the conservation of the total energy E. Equations (1a)-(1e) are closed with the following equation of state

$$p = \sum_{k=1}^{5} \frac{\rho_k}{\mathcal{M}_k}\mathcal{R}T$$

where p denotes the pressure, $\mathcal{R} = 8.3143J/(molK)$ is the universal gas constant and T is the translational temperature satisfying the following relation (Candler, 1988; Häuser *et al.*, 1989):

$$E = T\sum_{k=1}^{5}\rho_k C_{vk} + \sum_{k=1}^{5}\rho_k h_k^{0K} + \sum_{j=1}^{3}\mathcal{E}_{\mathbf{v}_j} + \rho\frac{v_x^2 + v_y^2}{2}$$

where h_k^{0K} is the heat of formation of specie k at the $0K$ reference temperature, and C_{vk} is the constant volume specific heat of specie k. Notice that C_{vk} are not the complete specific heats at constant volume, but they are only the part due to molecular translation and rotation, and they are constants. They take the value $C_{vk} = 2.5\mathcal{R}/\mathcal{M}_k$ for the diatomic specie, while $C_{vk} = 1.5\mathcal{R}/\mathcal{M}_k$ for the monatomic specie (Candler, 1988).

Remark 1. System (1a)-(1e) can be written as

$$\frac{\partial}{\partial t}\iint_{\mathcal{S}} \mathbf{U}\,d\mathcal{S} + \oint_{\partial\mathcal{S}} \left[F_x(\mathbf{U})n_x + F_y(\mathbf{U})n_y\right]\,d\ell = \iint_{\mathcal{S}} \mathbf{Z}(\mathbf{U})\,d\mathcal{S} \qquad (2)$$

where

$$\mathbf{U} = \begin{bmatrix} \rho_1 \\ \rho_2 \\ \rho_3 \\ \rho_4 \\ \rho_5 \\ \mathcal{E}_{v1} \\ \mathcal{E}_{v2} \\ \mathcal{E}_{v3} \\ m_x \\ m_y \\ E \end{bmatrix}, \quad F_x(\mathbf{U}) = \begin{bmatrix} \rho_1 v_x \\ \rho_2 v_x \\ \rho_3 v_x \\ \rho_4 v_x \\ \rho_5 v_x \\ \mathcal{E}_{v1} v_x \\ \mathcal{E}_{v2} v_x \\ \mathcal{E}_{v3} v_x \\ \rho v_x^2 + p \\ \rho v_x v_y \\ (E+p) v_x \end{bmatrix}, \quad F_y(\mathbf{U}) = \begin{bmatrix} \rho_1 v_y \\ \rho_2 v_y \\ \rho_3 v_y \\ \rho_4 v_y \\ \rho_5 v_y \\ \mathcal{E}_{v1} v_y \\ \mathcal{E}_{v2} v_y \\ \mathcal{E}_{v3} v_y \\ \rho v_x v_y \\ \rho v_y^2 + p \\ (E+p) v_y \end{bmatrix}, \quad \mathbf{Z}(\mathbf{U}) = \begin{bmatrix} W_1 \\ W_2 \\ W_3 \\ W_4 \\ W_5 \\ H_1 \\ H_2 \\ H_3 \\ 0 \\ 0 \\ 0 \end{bmatrix}$$

and

$$H_j = \frac{\mathcal{E}_{eq_j} - \mathcal{E}_{v_j}}{\tau_j} + \frac{W_j^+}{\rho_j}\mathcal{E}_{eq_j} + \frac{W_j^-}{\rho_j}\mathcal{E}_{v_j}, \tag{3}$$

with $j = 1, 2, 3$.

The Dunn and Kang and Park air model

The chemical reactions are modelled by the Dunn and Kang or Park air model (Park, 1984; 1985; Yu *et al.*, 1988), in which the ions, the free electron and the associated reactions are not included. This model comprises 17 elementary reactions (15 dissociation/recombination reactions and two exchange reactions) among the five specie N_2, O_2, NO, N and O. The chemical reactions considered in the model are:

$$N_2 + M \rightleftharpoons 2N + M$$

$$O_2 + M \rightleftharpoons 2O + M$$

$$NO + M \rightleftharpoons N + O + M$$

$$N_2 + O \rightleftharpoons NO + N$$

$$NO + O \rightleftharpoons O_2 + N$$

where M represents a collision partner or catalytic molecule; it can be any one of the five specie.

Remark 2. The Dunn and Kang or Park air model can be written as

$$\mathbf{W}(\mathbf{U}) = \sum_{j=1}^{5} f_j(\mathbf{U})\mathbf{v}_j - \sum_{j=1}^{5} b_j(\mathbf{U})\mathbf{v}_j$$

where $\mathbf{W}(\mathbf{U}) = [W_1, W_2, W_3, W_4, W_5]^{\mathrm{T}}$ and

$$\mathbf{v}_1 = \begin{bmatrix} -\mathcal{M}_1 \\ 0 \\ 0 \\ 2\mathcal{M}_4 \\ 0 \end{bmatrix}, \mathbf{v}_2 = \begin{bmatrix} 0 \\ -\mathcal{M}_2 \\ 0 \\ 0 \\ 2\mathcal{M}_5 \end{bmatrix}, \mathbf{v}_3 = \begin{bmatrix} 0 \\ 0 \\ -\mathcal{M}_3 \\ \mathcal{M}_4 \\ \mathcal{M}_5 \end{bmatrix}, \mathbf{v}_4 = \begin{bmatrix} -\mathcal{M}_1 \\ 0 \\ \mathcal{M}_3 \\ \mathcal{M}_4 \\ -\mathcal{M}_5 \end{bmatrix}, \mathbf{v}_5 = \begin{bmatrix} 0 \\ \mathcal{M}_2 \\ -\mathcal{M}_3 \\ \mathcal{M}_4 \\ -\mathcal{M}_5 \end{bmatrix}.$$

The forward and backward reaction rates are given by

$$f_1(\mathbf{U}) = \frac{\Gamma_1}{\mathcal{M}_1}\rho_1, \qquad b_1(\mathbf{U}) = \frac{\Omega_1}{\mathcal{M}_4^2}\rho_4^2$$

$$f_2(\mathbf{U}) = \frac{\Gamma_2}{\mathcal{M}_2}\rho_2, \qquad b_2(\mathbf{U}) = \frac{\Omega_2}{\mathcal{M}_5^2}\rho_5^2$$

$$f_3(\mathbf{U}) = \frac{\Gamma_3}{\mathcal{M}_3}\rho_3, \qquad b_3(\mathbf{U}) = \frac{\Omega_3}{\mathcal{M}_4\mathcal{M}_5}\rho_4\rho_5$$

$$f_4(\mathbf{U}) = \frac{\mathbf{K}_{f4}}{\mathcal{M}_1\mathcal{M}_5}\rho_1\rho_5, \qquad b_4(\mathbf{U}) = \frac{\mathbf{K}_{b4}}{\mathcal{M}_3\mathcal{M}_4}\rho_3\rho_4$$

$$f_5(\mathbf{U}) = \frac{\mathbf{K}_{f5}}{\mathcal{M}_3\mathcal{M}_5}\rho_3\rho_5, \qquad b_5(\mathbf{U}) = \frac{\mathbf{K}_{b5}}{\mathcal{M}_2\mathcal{M}_4}\rho_2\rho_4$$

where we have set

$$\Gamma_j = \sum_{m=1}^{5} \mathbf{K}_{fj,m}\frac{\rho_m}{\mathcal{M}_m}, \qquad \Omega_j = \sum_{m=1}^{5} \mathbf{K}_{bj,m}\frac{\rho_m}{\mathcal{M}_m},$$

with $j = 1, 2, 3$.

Remark 3. The reaction rates $\mathbf{K}_f$ and $\mathbf{K}_b$ are assumed to be functions of T, T_{v1}, T_{v2}, T_{v3} and they are described by the modified forms of the Arrhenius equation. These reaction rates K_f, K_b take the functional form

$$\kappa T_s^{\theta} \exp\left(-\frac{T_a}{T_s}\right)$$

where T_s is a function of the translational and vibrational temperatures and κ, θ, T_a are coefficients that depend on the specific reaction. The values of the coefficients κ, θ, T_a and the precise form of the function T_s for each reaction can be found in Candler (1988); Park (1985); Yu *et al.* (1988).

In the case of the Park air model the backward reaction rates are determined via the equilibrium constant $\mathbf{K}_E$, which are obtained by using a fourth-order polynomial fit of experimental spectroscopic data:

$$\mathrm{K}_b = \frac{\mathrm{K}_f}{\mathrm{K}_E}, \qquad \mathrm{K}_E(T) = exp\left(A_1 + A_2 Z + A_3 Z^2 + A_4 Z^3 + A_5 Z^4\right)$$

where $Z = 10000/T$. The coefficients A_i can be found in (Candler, 1988; Park, 1985).

Remark 4. Notice that the nitrogen mass fraction of the molecule *NO* is given by

$$\alpha = \frac{\mathcal{M}_4}{\mathcal{M}_4 + \mathcal{M}_5}$$

so that, by denoting with ρ_n the density of total mass of nitrogen and with ρ the density of total mass of oxygen, we have

$$\rho_N = \rho_1 + \alpha\rho_3 + \rho_4, \qquad \rho_O = \rho_2 + (1-\alpha)\rho_3 + \rho_5.$$

Since ρ_N and ρ_0 are conserved quantities, it follows that

$$\begin{bmatrix} 1 \\ 0 \\ \alpha \\ 1 \\ 0 \end{bmatrix} \cdot \mathbf{W}(\mathbf{U}) = 0, \qquad \begin{bmatrix} 0 \\ 1 \\ 1-\alpha \\ 0 \\ 1 \end{bmatrix} \cdot \mathbf{W}(\mathbf{U}) = 0.$$

Remark 5. Defining

$$\mathbf{R} = \left[\Gamma_1, \Gamma_2, \Gamma_3, \Omega_1, \Omega_2, \Omega_3, \mathrm{K}_{f_4}, \mathrm{K}_{f_5}, \mathrm{K}_{b4}, \mathrm{K}_{b5}\right]^T$$

and the vector of densities

$$\boldsymbol{\rho} = \left[\rho_1, \rho_2, \rho_3, \rho_4, \rho_5\right]^T$$

the source term $\mathbf{W}(\mathbf{U})$ can be expressed as a function of ρ and $\mathbf{R}$. In the appendix it is shown that the source terms $\mathbf{W}(\mathbf{U}) = \mathbf{W}(\rho, \mathbf{R})$ can be written in the form $\mathbf{C}(\rho, \mathbf{R})\rho$, where $\mathbf{C}(\rho, \mathbf{R})$ is a 5×5 matrix with continuous entries $C_{i,j}(\rho, \mathbf{R})$, such that:

(a) $C_{i,i}(\boldsymbol{\rho}, \mathbf{R}) \leq 0 \qquad i = 1, 2, 3, 4, 5$

(b) $C_{i,j}(\boldsymbol{\rho}, \mathbf{R}) \geq 0 \qquad i \neq j$

(c) $$\sum_{i=1}^{5} C_{i,j}(\rho, \mathbf{R}) = 0 \qquad j = 1,2,3,4,5$$

The partial fluxes

The flux in the direction **n** is given by

$$\mathbf{F}(\mathbf{U}, \mathbf{n}) = F_x(\mathbf{U})n_x + F_y(\mathbf{U})n_y, \tag{4}$$

and, due to the homogeneity of **F**, it satisfies

$$\mathbf{F}(\mathbf{U}, \mathbf{n}) = \mathbf{J}(\mathbf{U}, \mathbf{n})\mathbf{U}, \qquad \mathbf{J}(\mathbf{U}, \mathbf{n}) = \frac{\partial \mathbf{F}(\mathbf{U}, \mathbf{n})}{\partial \mathbf{U}},$$

where **J**(**U**, **n**) is the Jacobian of **F** with respect to **U**.

Remark 6. The homogeneous property of the flux **F** will be used to develop a flux vector splitting

$$\mathbf{F}(\mathbf{U}, \mathbf{n}) = \mathbf{F}^{+}(\mathbf{U}, \mathbf{n}) + \mathbf{F}^{-}(\mathbf{U}, \mathbf{n}),$$

where

$$\mathbf{F}^{\pm}(\mathbf{U}, \mathbf{n}) = \mathbf{A}^{\pm}(\mathbf{U}, \mathbf{n})\mathbf{U}, \tag{5}$$

with $\mathbf{A}^{+}$ and $\mathbf{A}^{-}$ square matrices. For a non-homogeneous flux, given $\mathbf{F}^{+}$ and $\mathbf{F}^{-}$ it is also possible to find some $\mathbf{A}^{+}$ and $\mathbf{A}^{-}$ which satisfy (5). This will permit to define a semi-implicit scheme analogous to the one developed here.

System (2) is hyperbolic and it is well known that the Jacobian **J**(**U**, **n**) has a complete set of eigenvectors with real eigenvalues (LeVeque, 1990), so that **J**(**U**, **n**) is diagonalizable as follows

$$\mathbf{J}(\mathbf{U}, \mathbf{n}) = \mathbf{X}(\mathbf{U}, \mathbf{n})\boldsymbol{\Lambda}(\mathbf{U}, \mathbf{n})\mathbf{X}(\mathbf{U}, \mathbf{n})^{-1}, \tag{6}$$

where

$$\boldsymbol{\Lambda}(\mathbf{U}, \mathbf{n}) = diag(\mathbf{v}\cdot\mathbf{n}, \mathbf{v}\cdot\mathbf{n}, \mathbf{v}\cdot\mathbf{n}, \mathbf{v}\cdot\mathbf{n}, \mathbf{v}\cdot\mathbf{n}, \mathbf{v}\cdot\mathbf{n}, \mathbf{v}\cdot\mathbf{n}, \mathbf{v}\cdot\mathbf{n}, \mathbf{v}\cdot\mathbf{n}, \mathbf{v}\cdot\mathbf{n} + c, \mathbf{v}\cdot\mathbf{n} - c),$$

is the eigenvalues matrix, moreover

$$c = \sqrt{\frac{1+\beta}{\rho}p}, \qquad \beta = \frac{\mathcal{R}\sum_{i=1}^{5}\frac{\rho_i}{\mathcal{M}_i}}{\sum_{i=1}^{5}\rho_i C_{vi}},$$

is the frozen speed of sound and **X**(**U**, **n**) is the right eigenvectors matrix. By using (6) equation (4) can be written as

$$\mathbf{F}(\mathbf{U}, \mathbf{n}) = (\mathbf{v}\cdot\mathbf{n})\mathcal{F}_{\mathbf{v}\cdot\mathbf{n}}(\mathbf{U}, \mathbf{n}) + (\mathbf{v}\cdot\mathbf{n} + c)\mathcal{F}_{\mathbf{v}\cdot\mathbf{n}+c}(\mathbf{U}, \mathbf{n}) + (\mathbf{v}\cdot\mathbf{n} - c)\mathcal{F}_{\mathbf{v}\cdot\mathbf{n}-c}(\mathbf{U}, \mathbf{n}),$$

where

$$\begin{aligned}
\mathcal{F}_{\mathbf{v}\cdot\mathbf{n}}(\mathbf{U},\mathbf{n}) &= \mathbf{X}(\mathbf{U},\mathbf{n})diag(1,1,1,1,1,1,1,1,1,0,0)\mathbf{X}(\mathbf{U},\mathbf{n})^{-1}\mathbf{U},\\
\mathcal{F}_{\mathbf{v}\cdot\mathbf{n}+c}(\mathbf{U},\mathbf{n}) &= \mathbf{X}(\mathbf{U},\mathbf{n})diag(0,0,0,0,0,0,0,0,0,1,0)\mathbf{X}(\mathbf{U},\mathbf{n})^{-1}\mathbf{U},\\
\mathcal{F}_{\mathbf{v}\cdot\mathbf{n}-c}(\mathbf{U},\mathbf{n}) &= \mathbf{X}(\mathbf{U},\mathbf{n})diag(0,0,0,0,0,0,0,0,0,0,1)\mathbf{X}(\mathbf{U},\mathbf{n})^{-1}\mathbf{U}.
\end{aligned} \tag{7}$$

The partial fluxes corresponding to each eigenvalue are defined as $\lambda \mathsf{F}_{\lambda}(\mathbf{U}, \mathbf{n})$, where λ takes the values $\mathbf{v}\cdot\mathbf{n}$, $\mathbf{v}\cdot\mathbf{n}+c$ and $\mathbf{v}\cdot\mathbf{n}-c$. Thus, the flux $\mathbf{F}(\mathbf{U}, \mathbf{n})$ is the sum of partial fluxes corresponding to each eigenvalue.

Remark 7. In order to define the numerical fluxes, the vector functions (7) can be rewritten as

$$\begin{cases}
\mathcal{F}_{\mathbf{v}\cdot\mathbf{n}}(\mathbf{U},\mathbf{n}) &= \dfrac{\beta\mathbf{U}}{1+\beta} + \mathcal{G}_{\mathbf{v}\cdot\mathbf{n}}(\mathbf{U},\mathbf{n})\\
\mathcal{F}_{\mathbf{v}\cdot\mathbf{n}+c}(\mathbf{U},\mathbf{n}) &= \dfrac{\mathbf{U}}{2(1+\beta)} + \mathcal{G}_{\mathbf{v}\cdot\mathbf{n}+c}(\mathbf{U},\mathbf{n})\\
\mathcal{F}_{\mathbf{v}\cdot\mathbf{n}-c}(\mathbf{U},\mathbf{n}) &= \dfrac{\mathbf{U}}{2(1+\beta)} + \mathcal{G}_{\mathbf{v}\cdot\mathbf{n}-c}(\mathbf{U},\mathbf{n})
\end{cases} \tag{8}$$

where

$$\begin{cases}
\mathcal{G}_{\mathbf{v}\cdot\mathbf{n}}(\mathbf{U},\mathbf{n}) &= \rho[0,0,0,0,0,0,0,0,0,0,-\kappa^2]^T\\
\mathcal{G}_{\mathbf{v}\cdot\mathbf{n}+c}(\mathbf{U},\mathbf{n}) &= \dfrac{\rho}{2}[0,0,0,0,0,0,0,0,\kappa n_x,\kappa n_y,\kappa^2+\kappa\mathbf{v}\cdot\mathbf{n}]^T\\
\mathcal{G}_{\mathbf{v}\cdot\mathbf{n}-c}(\mathbf{U},\mathbf{n}) &= \dfrac{\rho}{2}[0,0,0,0,0,0,0,0,-\kappa n_x,-\kappa n_y,\kappa^2-\kappa\mathbf{v}\cdot\mathbf{n}]^T
\end{cases}$$

and

$$\kappa = \frac{c}{1+\beta}.$$

Construction of the numerical flux

The numerical scheme to be developed for system (2) is obtained by a flux vector splitting technique. Therefore, the flux $\mathbf{F}(\mathbf{U}, \mathbf{n})$ will be split in the sum of a positive and a negative flux

$$\mathbf{F}(\mathbf{U},\mathbf{n}) = \mathbf{F}^{+}(\mathbf{U},\mathbf{n}) + \mathbf{F}^{-}(\mathbf{U},\mathbf{n}).$$

The positive and negative fluxes are defined as

$$\mathbf{F}^{+}(\mathbf{U},\mathbf{n}) = (\mathbf{v}\cdot\mathbf{n})^{+}\mathcal{F}_{\mathbf{v}\cdot\mathbf{n}}(\mathbf{U},\mathbf{n}) + (\mathbf{v}\cdot\mathbf{n}+c)^{+}\mathcal{F}_{\mathbf{v}\cdot\mathbf{n}+c}(\mathbf{U},\mathbf{n}) + (\mathbf{v}\cdot\mathbf{n}-c)^{+}\mathcal{F}_{\mathbf{v}\cdot\mathbf{n}-c}(\mathbf{U},\mathbf{n}),$$

$$\mathbf{F}^{-}(\mathbf{U},\mathbf{n}) = (\mathbf{v}\cdot\mathbf{n})^{-}\mathcal{F}_{\mathbf{v}\cdot\mathbf{n}}(\mathbf{U},\mathbf{n}) + (\mathbf{v}\cdot\mathbf{n}+c)^{-}\mathcal{F}_{\mathbf{v}\cdot\mathbf{n}+c}(\mathbf{U},\mathbf{n}) + (\mathbf{v}\cdot\mathbf{n}-c)^{-}\mathcal{F}_{\mathbf{v}\cdot\mathbf{n}-c}(\mathbf{U},\mathbf{n}),$$

where

$$(\mathbf{v}\cdot\mathbf{n})^+ = \max(0,\mathbf{v}\cdot\mathbf{n}), \qquad (\mathbf{v}\cdot\mathbf{n})^- = \min(0,\mathbf{v}\cdot\mathbf{n}),$$
$$(\mathbf{v}\cdot\mathbf{n}+c)^+ = \max(0,\mathbf{v}\cdot\mathbf{n}+c), \qquad (\mathbf{v}\cdot\mathbf{n}+c)^- = \min(0,\mathbf{v}\cdot\mathbf{n}+c),$$
$$(\mathbf{v}\cdot\mathbf{n}-c)^+ = \max(0,\mathbf{v}\cdot\mathbf{n}-c), \qquad (\mathbf{v}\cdot\mathbf{n}-c)^- = \min(0,\mathbf{v}\cdot\mathbf{n}-c),$$

as suggested in Steger and Warming (1981). Next, by equation (8), the positive flux can be rewritten as follows:

$$\mathbf{F}^+(\mathbf{U},\mathbf{n}) = \mathbf{a}_0(\mathbf{U},\mathbf{n})\mathbf{U} + \mathbf{G}^+(\mathbf{U},\mathbf{n}), \tag{9}$$

where

$$\mathbf{G}^+(\mathbf{U},\mathbf{n}) = (\mathbf{v}\cdot\mathbf{n})^+\mathcal{G}_{\mathbf{v}\cdot\mathbf{n}}(\mathbf{U},\mathbf{n}) + (\mathbf{v}\cdot\mathbf{n}+c)^+\mathcal{G}_{\mathbf{v}\cdot\mathbf{n}+c}(\mathbf{U},\mathbf{n}) + (\mathbf{v}\cdot\mathbf{n}-c)^+\mathcal{G}_{\mathbf{v}\cdot\mathbf{n}-c}(\mathbf{U},\mathbf{n}),$$
$$= \rho a_1(\mathbf{U},\mathbf{n})[0,\ldots,0,n_x,n_y,\mathbf{v}\cdot\mathbf{n}]^T + \rho a_2(\mathbf{U},\mathbf{n})[0,\ldots,0,1]^T,$$

and the non negative functions

$$a_0(\mathbf{U},\mathbf{n}) = \frac{\beta}{2(1+\beta)}\left(2(\mathbf{v}\cdot\mathbf{n}+c)^+ + (\mathbf{v}\cdot\mathbf{n}-c)^+ + 2(\mathbf{v}\cdot\mathbf{n})^+\right),$$
$$a_1(\mathbf{U},\mathbf{n}) = \frac{\kappa}{2}\left((\mathbf{v}\cdot\mathbf{n}+c)^+ - (\mathbf{v}\cdot\mathbf{n}-c)^+\right),$$
$$a_2(\mathbf{U},\mathbf{n}) = \frac{\kappa^2}{2}\left((\mathbf{v}\cdot\mathbf{n}+c)^+ + (\mathbf{v}\cdot\mathbf{n}-c)^+ - 2(\mathbf{v}\cdot\mathbf{n})^+\right), \tag{10}$$

are introduced for convenience.

Finite volume formulation

The finite volume numerical scheme proposed in this paper can be developed for a general unstructured grid. However, we restrict our attention here to grids arising from partitions of the plane into non-overlapping quadrilaterals of finite area (see Figure 1). Each quadrilateral is labelled by an integer coordinate pair as (i, j), the edge in common between the quadrilaterals (i, j) and $(i + 1, j)$ is labelled by $(i + 1/2, j)$ and the edge in common between the quadrilaterals (i, j) and $(i, j + 1)$ is labelled by $(i, j + 1/2)$. Next, $l_{i+1/2,j}$ is defined as the length of the edge $(i + 1/2, j)$ and $l_{i,j+1/2}$ is defined as the length of the edge $(i, j + 1/2)$. Finally, $S_{i,j}$ is the area of the quadrilateral (i, j). The vector $\mathbf{n}_{i+1/2,j}$ denotes the outer normal to the edge $(i + 1/2, j)$ of the cell (i, j) and similarly $\mathbf{n}_{i,j+1/2}$ denotes the outer normal to edge $(i, j + 1/2)$ of the cell (i, j). The semi-discrete finite volume approximation of system (2) can be written as

$$S_{i,j}\frac{\partial \mathbf{U}_{i,j}}{\partial t} + l_{i+1/2,j}\mathbf{F}(\mathbf{U}_{i,j},\mathbf{U}_{i+1,j},\mathbf{n}_{i+1/2,j}) + l_{i,j+1/2}\mathbf{F}(\mathbf{U}_{i,j},\mathbf{U}_{i,j+1},\mathbf{n}_{i,j+1/2})$$
$$+ l_{i-1/2,j}\mathbf{F}(\mathbf{U}_{i,j},\mathbf{U}_{i-1,j},-\mathbf{n}_{i-1/2,j}) + l_{i,j-1/2}\mathbf{F}(\mathbf{U}_{i,j},\mathbf{U}_{i,j-1},-\mathbf{n}_{i,j-1/2}) = S_{i,j}\mathbf{Z}(\mathbf{U}_{i,j}) \tag{11}$$

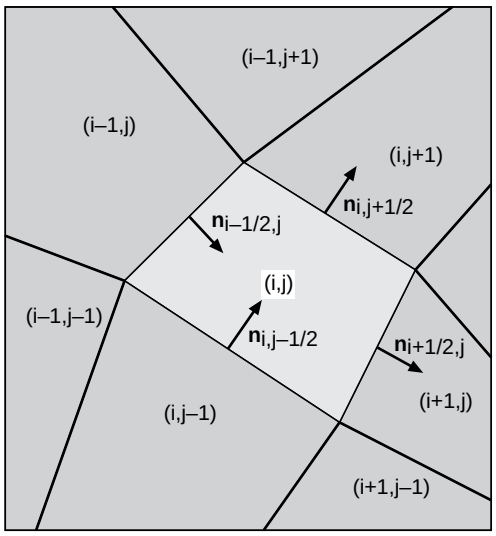

Figure 1.
Space grid

where $i = 1, 2, \ldots, N_x$, $j = 1, 2, \ldots, N_y$, $\mathbf{U}_{i,j}$ is an approximation of the mean value of **U** inside the cell (i, j).

Remark 8. The functions $\mathbf{F}(\mathbf{U}, \mathbf{V}, \mathbf{n})$ are approximations of the edge fluxes. For internal edges these functions are taken to be

$$\mathbf{F}(\mathbf{U}, \mathbf{V}, \mathbf{n}) = \mathbf{F}^+(\mathbf{U}, \mathbf{n}) + \mathbf{F}^-(\mathbf{V}, \mathbf{n}) = \mathbf{F}^+(\mathbf{U}, \mathbf{n}) - \mathbf{F}^+(\mathbf{V}, -\mathbf{n}), \quad (12)$$

namely, they are as in the standard upwind technique (LeVeque, 1990). For border edges the fluxes $\mathbf{F}(\mathbf{U}, \mathbf{V}, \mathbf{n})$ must be modified in order to satisfy the boundary conditions.

Finite volume scheme for densities

Any standard methods could be used for the time discretization of the ordinary differential system (11), unfortunately, explicit schemes have severe time step limitations, whereas fully implicit schemes lead to the solution of large nonlinear systems. The approach followed in this paper consists in using a semi-implicit scheme, where only a few terms are discretized implicitly in time. Denoting by

$$\mathbf{U}|_{[1,5]} = [U_1, U_2, U_3, U_4, U_5]^T,$$

the vector of the first five components of **U**, we can write the first five components of the flux $\mathbf{F}(\mathbf{U}, \mathbf{V}, \mathbf{n})$ by using equations (12), (9) and (10) as follows

$$\mathbf{F}|_{[1,5]}(\mathbf{U}, \mathbf{V}, \mathbf{n}) = \mathbf{a}_0(\mathbf{U}, \mathbf{n})\mathbf{U}|_{[1,5]} - \mathbf{a}_0(\mathbf{V}, -\mathbf{n})\mathbf{V}|_{[1,5]}.$$

By using the fact that $\mathbf{U}|_{[1,5]} + \rho$ and remark 5 the source term $\mathbf{Z}(\mathbf{U})$ for the first five components can be written as

$$\mathbf{Z}|_{[1,5]}(\mathbf{U}) = \mathbf{C}(\boldsymbol{\rho}, \mathbf{R})\boldsymbol{\rho}.$$

Then, the system (11) for the first five components takes the form

$$\mathcal{S}_{i,j}\frac{\partial \boldsymbol{\rho}_{i,j}}{\partial t} + e_{i,j}\boldsymbol{\rho}_{i,j} - a_{i-1,j}\boldsymbol{\rho}_{i-1,j} - b_{i+1,j}\boldsymbol{\rho}_{i+1,j} - c_{i,j-1}\boldsymbol{\rho}_{i,j-1} - d_{i,j+1}\boldsymbol{\rho}_{i,j+1} = \mathcal{S}_{i,j}\mathbf{C}(\boldsymbol{\rho}_{i,j}, \mathbf{R}_{i,j})\boldsymbol{\rho}_{i,j},$$

where

$$\begin{aligned}
a_{i,j} &= \ell_{i+1/2,j}\mathrm{a}_0(\mathbf{U}_{i,j}, \mathbf{n}_{i+1/2,j}),\\
b_{i,j} &= \ell_{i-1/2,j}\mathrm{a}_0(\mathbf{U}_{i,j}, -\mathbf{n}_{i-1/2,j}),\\
c_{i,j} &= \ell_{i,j+1/2}\mathrm{a}_0(\mathbf{U}_{i,j}, \mathbf{n}_{i,j+1/2}),\\
d_{i,j} &= \ell_{i,j-1/2}\mathrm{a}_0(\mathbf{U}_{i,j}, -\mathbf{n}_{i,j-1/2}),\\
e_{i,j} &= a_{i,j} + b_{i,j} + c_{i,j} + d_{i,j},
\end{aligned} \tag{13}$$

are non negative numbers. Using forward finite difference to approximate $d\rho_{i,j}/dt$ and computing $a_{i,j}$, $b_{i,j}$, $c_{i,j}$ and $d_{i,j}$ at the time step n, the semi-implicit scheme for the densities is obtained. The resulting scheme can be written as

$$\begin{aligned}
&\left(\frac{\mathcal{S}_{i,j}}{\Delta t} + e^n_{i,j}\right)\boldsymbol{\rho}^{n+1}_{i,j} - a^n_{i-1,j}\boldsymbol{\rho}^{n+1}_{i-1,j} - b^n_{i+1,j}\boldsymbol{\rho}^{n+1}_{i+1,j} - c^n_{i,j-1}\boldsymbol{\rho}^{n+1}_{i,j-1} - d^n_{i,j+1}\boldsymbol{\rho}^{n+1}_{i,j+1}\\
&\qquad = \mathcal{S}_{i,j}\mathbf{C}(\boldsymbol{\rho}^{n+1}_{i,j}, \mathbf{R}^n_{i,j})\boldsymbol{\rho}^{n+1}_{i,j} + \frac{\mathcal{S}_{i,j}}{\Delta t}\boldsymbol{\rho}^n_{i,j}.
\end{aligned} \tag{14}$$

The system (14) can be written in *stencil* notation as

$$-\mathcal{S}_{i,j}\mathbf{C}(\boldsymbol{\rho}^{n+1}_{i,j}, \mathbf{R}^n_{i,j})\boldsymbol{\rho}^{n+1}_{i,j} + \begin{pmatrix} & -d^n_{i,j+1} & \\ -a^n_{i-1,j} & \frac{\mathcal{S}_{i,j}}{\Delta t} + e^n_{i,j} & -b^n_{i+1,j} \\ & -c^n_{i,j-1} & \end{pmatrix}\boldsymbol{\rho}^{n+1}_{i,j} = \frac{\mathcal{S}_{i,j}}{\Delta t}\boldsymbol{\rho}^n_{i,j}. \tag{15}$$

An appropriate choice of the edge fluxes in the following four boundaries

$$\begin{aligned}
\partial_{\text{left}} &= \{(1/2, j)\,|\,j = 1, 2, \ldots, N_y\},\\
\partial_{\text{right}} &= \{(N_x + 1/2, j)\,|\,j = 1, 2, \ldots, N_y\},\\
\partial_{\text{down}} &= \{(i, 1/2)\,|\,i = 1, 2, \ldots, N_x\},\\
\partial_{\text{up}} &= \{(i, N_y + 1/2)\,|\,i = 1, 2, \ldots, N_x\},
\end{aligned}$$

is now necessary in order to close system (15). Without loss of generality, only the flux at the border ∂_{left} is considered (see Figure 2). So it is enough to find an appropriate discretization for

$$\ell_{1/2,j}\mathbf{F}|_{[1,5]}(\mathbf{U}_{0,j}, \mathbf{U}_{1,j}, -\mathbf{n}_{1/2,j}).$$

We now consider various possible cases:

Solid boundary

In the case of solid boundary we apply the usual condition $\mathbf{v} \cdot \mathbf{n} = 0$, so that, the fluxes $\mathbf{F}(\mathbf{U}, \mathbf{n})$ for the first five components become

$$\mathbf{F}|_{[1,5]}(\mathbf{U}, \mathbf{n}) = \rho \mathbf{v} \cdot \mathbf{n} = 0,$$

and system (15) at the left boundary becomes

$$-\mathcal{S}_{1,j}\mathbf{C}(\boldsymbol{\rho}_{1,j}^{n+1}, \mathbf{R}_{1,j}^{n})\boldsymbol{\rho}_{1,j}^{n+1} + \begin{pmatrix} & -d_{1,j+1}^{n} & \\ & \dfrac{\mathcal{S}_{1,j}}{\Delta t} + e_{1,j}^{(1)} & -b_{1+1,j}^{n} \\ & -c_{1,j-1}^{n} & \end{pmatrix} \boldsymbol{\rho}_{1,j}^{n+1} = \frac{\mathcal{S}_{1,j}}{\Delta t}\boldsymbol{\rho}_{1,j}^{n},$$

where $e_{i,j}^{(1)} = a_{i,j}^{n} + c_{i,j}^{n} + d_{i,j}^{n}$.

Supersonic inlet

All the characteristics are incoming and we must specify the external quantities. In this case $\mathbf{F}|_{[1,5]}(\mathbf{U}_{0,j}, \mathbf{U}_{1,j}, -\mathbf{n}_{1/2,j}) = -\rho_{0,j}\mathbf{v}_{0,j} \cdot \mathbf{n}_{1/2,j} < 0$ and system (15) becomes

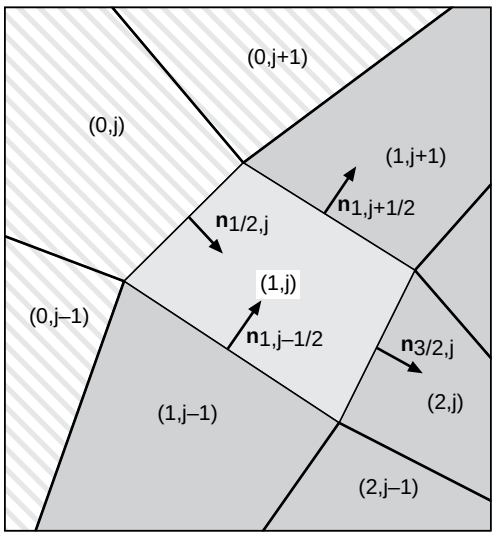

Figure 2.
Left border

$$-\mathcal{S}_{1,j}\mathbf{C}(\boldsymbol{\rho}_{1,j}^{n+1},\mathbf{R}_{1,j}^{n})\boldsymbol{\rho}_{1,j}^{n+1}+\begin{pmatrix} & -d_{1,j+1}^{n} & \\ \hline & \dfrac{\mathcal{S}_{1,j}}{\Delta t}+e_{1,j}^{(1)} & -b_{1+1,j}^{n} \\ \hline & -c_{1,j-1}^{n} & \end{pmatrix}\boldsymbol{\rho}_{1,j}^{n+1}$$

$$=\frac{\mathcal{S}_{1,j}}{\Delta t}\boldsymbol{\rho}_{1,j}^{n}+\ell_{1/2,j}\rho_{0,j}\mathbf{v}_{0,j}\cdot\mathbf{n}_{1/2,j}.$$

Free outlet

In this case the flux depends only on the internal quantities, $\mathbf{F}|_{[1,5]}(\mathbf{U}_{0,j}, \mathbf{U}_{1,j}, -\mathbf{n}_{1/2,j}) = -\rho_{0,j}\,\mathbf{v}_{1,j}\cdot\mathbf{n}_{1/2,j} > 0$ and system (15) becomes

$$-\mathcal{S}_{1,j}\mathbf{C}(\boldsymbol{\rho}_{1,j}^{n+1},\mathbf{R}_{1,j}^{n})\boldsymbol{\rho}_{1,j}^{n+1}+\begin{pmatrix} & -d_{1,j+1}^{n} & \\ \hline & \dfrac{\mathcal{S}_{1,j}}{\Delta t}+e_{1,j}^{(2)} & -b_{1+1,j}^{n} \\ \hline & -c_{1,j-1} & \end{pmatrix}\boldsymbol{\rho}_{1,j}^{n+1}=\frac{\mathcal{S}_{1,j}}{\Delta t}\boldsymbol{\rho}_{1,j}^{n},$$

where $e_{1,j}^{(2)}+e_{1,j}^{(1)}-\ell_{1/2,j}\nu_{1,j}\cdot\mathbf{n}_{1/2,j}$.

Remark 9. In general, the system (15) with boundary conditions becomes

$$-\mathcal{S}_{i,j}\mathbf{C}(\boldsymbol{\rho}_{i,j}^{n+1},\mathbf{R}_{i,j}^{n})\boldsymbol{\rho}_{i,j}^{n+1}+\begin{pmatrix} & -d_{i,j+1}^{n} & \\ \hline -a_{i-1,j}^{n} & \dfrac{\mathcal{S}_{i,j}}{\Delta t}+e_{i,j}^{n} & -b_{i+1,j}^{n} \\ \hline & -c_{i,j-1}^{n} & \end{pmatrix}\boldsymbol{\rho}_{i,j}^{n+1}=\frac{\mathcal{S}_{i,j}}{\Delta t}\boldsymbol{\rho}_{i,j}^{n}+\mathrm{bc}_{i,j}^{n},$$

where $\mathrm{bc}_{i,j}^{n} \geq 0$ and it is non zero only at the boundary, and $a_{i,j}^{n}, b_{i,j}^{n}, c_{i,j}^{n}, d_{i,j}^{n} \geq 0$. Here, $a_{i,j}^{n}, b_{i,j}^{n}, c_{i,j}^{n}$, and $d_{i,j}^{n}$ are as in (13) (with $\mathbf{U}$ evaluated at time step n) and must be eventually modified at the boundary.

These semi-implicit formulations of the boundary conditions allow us to prove the non-negativity of the densities and of the vibrational energies.

Equations (15) constitute a 5 by 5 block five-diagonal system, in which only the main diagonal blocks $\mathbf{C}(\rho, \mathbf{R}_{i,j}^{n})$ are nonlinear. The solution of the nonlinear system (15) allows to compute $\rho_{i,j}^{n+1}$, so that a decoupling of the densities from the other discretized quantities results.

Remark 10. The system of equations (15) will be solved by an iterative procedure. Observe that system (15) can be written as $\mathbf{D}(x)x + \mathbf{M}x = b$ where

$\mathbf{D}(x) = diag(-\mathbf{C}(x_{i,j}, \mathbf{R}_{i,j}^{n+1}))$. The solution x will be the value of ρ^{n+1}. A convenient solution technique is the following Jacoby-type iteration

$$(\Gamma + \mathbf{D}(\mathbf{x}^s) + \mathbf{M})\mathbf{x}^{s+1} = \Gamma\mathbf{x}^s + \mathbf{b},$$

where the diagonal matrix Γ improves the condition number of the iteration matrix $[\Gamma + \mathbf{D}(x^S) + \mathbf{M}]^{-1}$. The iterative process is described in Table I.

For the procedure described in Table I the following results are proved in the Appendix.

(1) The quantities defined by the iterative procedure of Table I are non-negative for all s. It follows that at convergence ρ^{n+1} is non-negative.

(2) The solution algorithm for system (15) conserves the total amount of nitrogen and oxygen. The conservation of the total amount of nitrogen and oxygen is essential in order to avoid spurious numerical transformation of nitrogen into oxygen and vice versa. The conservation of these quantities is used in stopping test for the iterations in Table I.

(3) For all $\Delta t > 0$ exists at least one non-negative solution of the non-linear system (15).

(4) If Δt is small enough, then solution of (15) is unique and the iterative process converges.

Remark 11. In practical computation instead of solving the linear system in Table I it is enough to approximate the solution with one or more iterations of a non-negative iterative scheme. The system in Table I can be written in the quasi two colour form (see Ortega (1988) for coloration):

$$\begin{bmatrix} \mathbf{D}_1(\mathbf{x}_1, \mathbf{x}_2) & -\mathbf{U} \\ -\mathbf{L} & \mathbf{D}_2(\mathbf{x}_1, \mathbf{x}_2) \end{bmatrix} \begin{bmatrix} \mathbf{x}_1 \\ \mathbf{x}_2 \end{bmatrix} = \begin{bmatrix} \mathbf{b}_1 \\ \mathbf{b}_2 \end{bmatrix},$$

(1) Set $\mathbf{x}_{i,j}^0 = \rho_{i,j}^n$

(2) For $s = 0, 1, 2, \ldots$ until convergence set $\mathbf{x}^{s+1} = \Phi(\mathbf{x}^s)$ where $\mathbf{x}^{s+1}$ is defined as the solution of the linear system

$$-\mathbf{C}(\mathbf{x}_{i,j}^s)\mathbf{x}_{i,j} + \begin{pmatrix} & -d_{i,j+1}^n & \\ -a_{i-1,j}^n & \Gamma_{i,j} + e_{i,j}^n & -b_{i+1,j}^n \\ & -c_{i,j-1}^n & \end{pmatrix} \mathbf{x}_{i,j} = \Gamma_{i,j}\mathbf{x}_{i,j}^s + \frac{\mathbf{S}_{i,j}}{\Delta t}\boldsymbol{\rho}_{i,j}^n.$$

(3) At convergence set $\rho_{i,j}^{n+1} = x_{i,j}^{s+1}$

Table I.
Densities solver

where $\mathbf{L}$, $U \geq 0$ and $\mathbf{D}_1(\mathbf{x}_1, \mathbf{x}_2)$, $\mathbf{D}_2(\mathbf{x}_1, \mathbf{x}_2)$ are M-matrices. A convenient iterative solution procedure is the following:

$$\begin{aligned}
\mathbf{L}^i &= \mathbf{D}_2(\mathbf{x}_1^i, \mathbf{x}_2^i)^{-1}\mathbf{L}, \\
\mathbf{U}^i &= \mathbf{D}_1(\mathbf{x}_1^i, \mathbf{x}_2^i)^{-1}\mathbf{U}, \\
\mathbf{x}_2^{i+1} &= \mathbf{b}_2 + \mathbf{L}^i(\mathbf{b}_1 + \mathbf{U}^i\mathbf{x}_2^i), \\
\mathbf{x}_1^{i+1} &= \mathbf{b}_1 + \mathbf{U}^i\mathbf{x}_2^{i+1},
\end{aligned} \tag{16}$$

and few iterations with (16) are enough for approximating the solution of the linear system. This solution procedure corresponds to a splitting scheme for $\mathbf{A}x = b$ as follows

$$\mathbf{x}^{i+1} = (\mathbf{I} - \mathbf{P}^{-1}\mathbf{A})\mathbf{x}^i + \mathbf{P}^{-1}\mathbf{b}.$$

Here,

$$\mathbf{A} = \begin{bmatrix} \mathbf{I} & -\mathbf{D}_1(\mathbf{x}_1, \mathbf{x}_2)^{-1}\mathbf{U} \\ -\mathbf{D}_2(\mathbf{x}_1, \mathbf{x}_2)^{-1}\mathbf{L} & \mathbf{I} \end{bmatrix},$$

$$\mathbf{b} = \begin{bmatrix} \mathbf{D}_1(\mathbf{x}_1, \mathbf{x}_2)^{-1}\mathbf{b}_1 \\ \mathbf{D}_2(\mathbf{x}_1, \mathbf{x}_2)^{-1}\mathbf{b}_2 \end{bmatrix},$$

$$\mathbf{P} = \begin{bmatrix} \mathbf{I} & 0 \\ -\mathbf{D}_2(\mathbf{x}_1, \mathbf{x}_2)^{-1}\mathbf{L} & \mathbf{I} \end{bmatrix} \begin{bmatrix} \mathbf{I} & -\mathbf{D}_1(\mathbf{x}_1, \mathbf{x}_2)^{-1}\mathbf{U} \\ 0 & \mathbf{I} \end{bmatrix}.$$

Remark 12. The scheme (15) is only first order in time accurate for the chemical source terms. It is possible to improve the time step accuracy with simple modifications. This possibility is examined in Bertolazzi (1996).

Finite volume scheme for vibrational energies

The time discretization of the equations for the vibrational energies can be developed along the same lines as for the densities. The flux $\mathbf{F}(\mathbf{U}, \mathbf{V}, \mathbf{n})$ for the sixth through eighth components becomes, by equations (12), (9) and (10)

$$\mathbf{F}|_{[6,8]}(\mathbf{U}, \mathbf{V}, \mathbf{n}) = a_0(\mathbf{U}, \mathbf{n})\mathbf{U}|_{[6,8]} - a_0(\mathbf{V}, -\mathbf{n})\mathbf{V}|_{[6,8]},$$

where $\mathbf{U}|_{[6,8]} + [E_{v1}, E_{v2}, E_{v3}]^T$. The source term $\mathbf{Z}(\mathbf{U})$ for the sixth through eighth components can be written by (3) as

$$\mathbf{Z}|_{[6,8]}(\mathbf{U}) = \begin{bmatrix} H_1 \\ H_2 \\ H_3 \end{bmatrix} = \begin{bmatrix} \dfrac{\mathcal{E}_{\mathrm{eq}_1} - \mathcal{E}_{\mathrm{v}1}}{\tau_1} + \dfrac{W_1^+}{\rho_1}\mathcal{E}_{\mathrm{eq}_1} + \dfrac{W_1^-}{\rho_1}\mathcal{E}_{\mathrm{v}1} \\ \dfrac{\mathcal{E}_{\mathrm{eq}_2} - \mathcal{E}_{\mathrm{v}2}}{\tau_2} + \dfrac{W_2^+}{\rho_2}\mathcal{E}_{\mathrm{eq}_2} + \dfrac{W_2^-}{\rho_2}\mathcal{E}_{\mathrm{v}2} \\ \dfrac{\mathcal{E}_{\mathrm{eq}_3} - \mathcal{E}_{\mathrm{v}3}}{\tau_3} + \dfrac{W_3^+}{\rho_3}\mathcal{E}_{\mathrm{eq}_3} + \dfrac{W_3^-}{\rho_3}\mathcal{E}_{\mathrm{v}3} \end{bmatrix}.$$

Therefore, the system (11) for the sixth through eighth components takes the form

$$\mathcal{S}_{i,j}\frac{\partial(\mathcal{E}_{\mathrm{v}k})_{i,j}}{\partial t} + e^n_{i,j}(\mathcal{E}_{\mathrm{v}k})_{i,j}$$

$$-a^n_{i-1,j}(\mathcal{E}_{\mathrm{v}k})_{i-1,j} - b^n_{i+1,j}(\mathcal{E}_{\mathrm{v}k})_{i+1,j} - c^n_{i,j-1}(\mathcal{E}_{\mathrm{v}k})_{i,j-1} - d^n_{i,j+1}(\mathcal{E}_{\mathrm{v}k})_{i,j+1}$$

$$= \mathcal{S}_{i,j}\left[\frac{(\mathcal{E}_{\mathrm{eq}_k})_{i,j} - (\mathcal{E}_{\mathrm{v}k})_{i,j}}{\tau_{k,i,j}} + \left(\frac{W_k^+}{\rho_k}\right)_{i,j}(\mathcal{E}_{\mathrm{eq}_k})_{i,j} + \left(\frac{W_k^-}{\rho_k}\right)_{i,j}(\mathcal{E}_{\mathrm{v}k})_{i,j}\right],$$

where $a_{i,j}$, $b_{i,j}$, $c_{i,j}$ and $d_{i,j}$ are defined in (13). Using forward finite difference to approximate $\mathbf{d}(\mathrm{Ev}_k)_{i,j}/dt$ and computing $a_{i,j}$, $b_{i,j}$, $c_{i,j}$ and $d_{i,j}$ at the time step n, a semi-implicit scheme for the vibrational energies is obtained

$$\left(\frac{\mathcal{S}_{i,j}}{\Delta t} + \frac{1}{(\tau_k)^n_{i,j}} - \left(\frac{\hat{W}_k^-}{\rho_k}\right)^{n+1}_{i,j} + e^n_{i,j}\right)(\mathcal{E}_{\mathrm{v}k})^{n+1}_{i,j}$$

$$-a^n_{i-1,j}(\mathcal{E}_{\mathrm{v}k})^{n+1}_{i-1,j} - b^n_{i+1,j}(\mathcal{E}_{\mathrm{v}k})^{n+1}_{i+1,j} - c^n_{i,j-1}(\mathcal{E}_{\mathrm{v}k})^{n+1}_{i,j-1} - d^n_{i,j+1}(\mathcal{E}_{\mathrm{v}k})^{n+1}_{i,j+1}$$

$$= \mathcal{S}_{i,j}\left\{\frac{(\mathcal{E}_{\mathrm{v}k})^n_{i,j}}{\Delta t} + \left(\frac{\mathcal{E}_{\mathrm{v}k}}{\rho_k}\right)^n_{i,j}\left[\left(\frac{\rho_k}{\tau_k}\right)^n_{i,j} + (\hat{W}_k^+)_{i,j}\right]\right\}. \tag{17}$$

Here we have defined

$$\hat{W}_{i,j} = \mathbf{C}(\boldsymbol{\rho}^{n+1}_{i,j}, \mathbf{R}^n_{i,j})\boldsymbol{\rho}^{n+1}_{i,j},$$

$$(\hat{W}_k^-)_{i,j} = C_{k,k}(\boldsymbol{\rho}^{n+1}_{i,j}, \mathbf{R}^n_{i,j})(\rho_k)^{n+1}_{i,j},$$

$$\hat{W}^+_{i,j} = \hat{W}_{i,j} - \hat{W}^-_{i,j}.$$

The boundary conditions are analogous to the boundary conditions for the densities.

Remark 13. As remarked for (15), system (17) can be written in stencil notation as

$$\begin{pmatrix} & -d^n_{i,j+1} & \\ -a^n_{i-1,j} & \delta_{i,j} & -b^n_{i+1,j} \\ & -c^n_{i,j-1} & \end{pmatrix} (\mathcal{E}_{\mathrm{v}k})^{n+1}_{i,j} = b_{i,j}, \tag{18}$$

where

$$\delta_{i,j} = \frac{\mathcal{S}_{i,j}}{\Delta t} + \frac{1}{\tau^n_{k,i,j}} - \left(\frac{\hat{W}^-_k}{\rho_k}\right)^{n+1}_{i,j} + e_{i,j},$$

$$b_{i,j} = \mathcal{S}_{i,j}\left\{\frac{(\mathcal{E}_{\mathrm{v}k})^n_{i,j}}{\Delta t} + \left(\frac{\mathcal{E}_{\mathrm{v}k}}{\rho_k}\right)^n_{i,j}\left[\left(\frac{\rho_k}{\tau_k}\right)^n_{i,j} + (\hat{W}^+_k)_{i,j}\right]\right\} + \mathrm{bc}^n_{i,j}.$$

It is proved in the Appendix that the solution of system (18) is non-negative. Notice that in equation (18) the vibrational energies Ev_k are mutually separated. Thus, three five-diagonal linear systems instead of one 3 by 3 block five-diagonal linear system must be solved.

Numerical scheme for energy and momenta terms

The positive flux of equation (11) for the three last components is given by

$$\mathbf{F}^+(\mathbf{U},\mathbf{n})|_{[9,11]} = \mathbf{a}_0(\mathbf{U},\mathbf{n})\begin{bmatrix} m_x \\ m_y \\ E \end{bmatrix} + \rho\mathbf{a}_1(\mathbf{U},\mathbf{n})\begin{bmatrix} n_x \\ n_y \\ \mathbf{v}\cdot\mathbf{n} \end{bmatrix} + \rho\mathbf{a}_2(\mathbf{U},\mathbf{n})\begin{bmatrix} 0 \\ 0 \\ 1 \end{bmatrix}.$$

Setting $\mathbf{X} = [m_x, m_y, E]^T$ the discretization of (2) for the last three components becomes

$$\left(\frac{\mathcal{S}_{i,j}}{\Delta t} + e^n_{i,j}\right)\mathbf{X}^{n+1}_{i,j} - a^n_{i-1,j}\mathbf{X}^{n+1}_{i-1,j} - b^n_{i+1,j}\mathbf{X}^{n+1}_{i+1,j}$$

$$-c^n_{i,j-1}\mathbf{X}^{n+1}_{i,j-1} - d^n_{i,j+1}\mathbf{X}^{n+1}_{i,j+1} = \frac{\mathcal{S}_{i,j}}{\Delta t}\mathbf{X}^n_{i,j} - \mathbf{r}_{i,j} \tag{19}$$

where

$$\mathbf{r}_{i,j} = \mathbf{f}_{i+1/2,j} - \mathbf{f}_{i-1/2,j} + \mathbf{f}_{i,j+1/2} - \mathbf{f}_{i,j-1/2},$$

$$\mathbf{f}_{i+1/2,j} = \rho^{n+1}_{i,j}\mathbf{a}^n_{i,j} - \rho^{n+1}_{i+1,j}\mathbf{b}^n_{i+1,j}, \qquad \mathbf{f}_{i,j+1/2} = \rho^{n+1}_{i,j}\mathbf{c}^n_{i,j} - \rho^{n+1}_{i,j+1}\mathbf{d}^n_{i,j+1},$$

and

$$\mathbf{a}_{i,j}^n = \ell_{i+1/2,j}\left(\mathbf{a}_1(\mathbf{U}_{i,j}^n, \mathbf{n}_{i+1/2,j})\begin{bmatrix}(n_x)_{i+1/2,j}\\(n_y)_{i+1/2,j}\\ \mathbf{v}_{i,j}\cdot\mathbf{n}_{i+1/2,j}\end{bmatrix} + \mathbf{a}_2(\mathbf{U}_{i,j}^n, \mathbf{n}_{i+1/2,j})\begin{bmatrix}0\\0\\1\end{bmatrix}\right),$$

$$\mathbf{b}_{i,j}^n = \ell_{i-1/2,j}\left(\mathbf{a}_1(\mathbf{U}_{i,j}^n, -\mathbf{n}_{i-1/2,j})\begin{bmatrix}(-n_x)_{i-1/2,j}\\(-n_y)_{i-1/2,j}\\ -\mathbf{v}_{i,j}\cdot\mathbf{n}_{i-1/2,j}\end{bmatrix} + \mathbf{a}_2(\mathbf{U}_{i,j}^n, -\mathbf{n}_{i-1/2,j})\begin{bmatrix}0\\0\\1\end{bmatrix}\right),$$

$$\mathbf{c}_{i,j}^n = \ell_{i,j+1/2}\left(\mathbf{a}_1(\mathbf{U}_{i,j}^n, \mathbf{n}_{i,j+1/2})\begin{bmatrix}(n_x)_{i,j+1/2}\\(n_y)_{i,j+1/2}\\ \mathbf{v}_{i,j}^n\cdot\mathbf{n}_{i,j+1/2}\end{bmatrix} + \mathbf{a}_2(\mathbf{U}_{i,j}, \mathbf{n}_{i,j+1/2})\begin{bmatrix}0\\0\\1\end{bmatrix}\right),$$

$$\mathbf{d}_{i,j}^n = \ell_{i,j-1/2}\left(\mathbf{a}_1(\mathbf{U}_{i,j}^n, -\mathbf{n}_{i,j-1/2})\begin{bmatrix}(-n_x)_{i,j-1/2}\\(-n_y)_{i,j-1/2}\\ -\mathbf{v}_{i,j}\cdot\mathbf{n}_{i,j-1/2}\end{bmatrix} + \mathbf{a}_2(\mathbf{U}_{i,j}^n, -\mathbf{n}_{i,j-1/2})\begin{bmatrix}0\\0\\1\end{bmatrix}\right),$$

In stencil notation system (19) becomes

$$\left(\begin{array}{c|c|c} & -d_{i,j+11} & \\ \hline -a_{i-1,j1} & \dfrac{\mathcal{S}_{i,j}}{\Delta t} + e_{i,j1} & -b_{i+1,j1} \\ \hline & -c_{i,j-11} & \end{array}\right)\mathbf{X}_{i,j}^{n+1} = \frac{\mathcal{S}_{i,j}}{\Delta t}\mathbf{X}_{i,j}^n - \mathbf{r}_{i,j}^n.$$

Notice that in equation (19) momenta m_x, m_y and total energy E are mutually separated. Thus, three five-diagonal linear systems instead of one 3 by 3 block five diagonal linear systems must be solved. At the boundary the matrices must be changed to satisfy boundary conditions. Here, without loss of generality, only the boundary conditions at ∂_{left} are considered (see Figure 2). So it is enough to find an appropriate discretization for

$$\ell_{1/2,j}\mathbf{F}|_{[9,11]}(\mathbf{U}_{0,j}, \mathbf{U}_{1,j}, -\mathbf{n}_{1/2,j}).$$

Solid boundary)

The fluxes $\mathbf{F}(\mathbf{U}, \mathbf{n})$ for the last three components are

$$\mathbf{F}|_{[9,11]}(\mathbf{U}, \mathbf{n}) = \mathbf{v}\cdot\mathbf{n}\begin{bmatrix}m_x\\m_y\\ \mathbf{v}\cdot\mathbf{n}\end{bmatrix} + \frac{\rho c^2}{1+\beta}\begin{bmatrix}n_x\\n_y\\ \mathbf{v}\cdot\mathbf{n}\end{bmatrix}.$$

In the case of solid boundary we have the usual condition $\mathbf{v}\cdot\mathbf{n} = 0$, so that

$$\mathbf{F}(\mathbf{U}_{0,j}, \mathbf{U}_{1,j}, -\mathbf{n}_{1/2,j}) = \frac{\rho_{1,j} c_{1,j}^2}{1+\beta_{1,j}} \begin{bmatrix} (-n_x)_{1/2,j} \\ (-n_y)_{1/2,j} \\ 0 \end{bmatrix}.$$

Supersonic inlet boundary

All the characteristic are inlet and we must specify the external quantities. In this case,

$$\mathbf{F}(\mathbf{U}_{0,j}, \mathbf{U}_{1,j}, -\mathbf{n}_{1/2,j}) = (-\mathbf{v}_{0,j} \cdot n_{1/2,j}) \begin{bmatrix} (m_x)_{0,j} \\ (m_y)_{0,j} \\ E_{0,j} \end{bmatrix} + \frac{\rho_{0,j} c_{0,j}^2}{1+\beta_{0,j}} \begin{bmatrix} (-n_x)_{1/2,j} \\ (-n_y)_{1/2,j} \\ (-\mathbf{v}_{0,j} \cdot n_{1/2,j}) \end{bmatrix}.$$

Free outlet

In this case the flux depends only of the internal quantities,

$$\mathbf{F}(\mathbf{U}_{0,j}, \mathbf{U}_{1,j}, -\mathbf{n}_{1/2,j}) = (-\mathbf{v}_{1,j} \cdot n_{1/2,j}) \begin{bmatrix} (m_x)_{1,j} \\ (m_y)_{1,j} \\ E_{1,j} \end{bmatrix} + \frac{\rho_{1,j} c_{1,j}^2}{1+\beta_{1,j}} \begin{bmatrix} (-n_x)_{1/2,j} \\ (-n_y)_{1/2,j} \\ (-\mathbf{v}_{1,j} \cdot n_{1/2,j}) \end{bmatrix}.$$

Second order in time accuracy

Equations (11) constitute a large system of ordinary differential equations in the unknowns $\mathbf{U}_{i,j}$. We can use any kind of standard solver for ODE, for example in the previous sections a semi-implicit version of Euler scheme was used. The previous scheme was only first order in time accurate, better accuracy can be reached using, for example, Runge-Kutta schemes. A second order in time scheme can be obtained estimating the coefficients of the linear and non-linear systems at time step $n + 1/2$ by using the previous scheme. The resulting scheme is very close to the scheme found in Collatz (1960) and for the densities results in the following scheme:

$$\begin{aligned} &\frac{\mathcal{S}_{i,j}}{\Delta t}(\boldsymbol{\rho}_{i,j}^{n+1} - \boldsymbol{\rho}_{i,j}^{n}) + e_{i,j}^{n+1/2} \frac{\boldsymbol{\rho}_{i,j}^{n+1} + \boldsymbol{\rho}_{i,j}^{n}}{2} \\ &- a_{i-1,j}^{n+1/2} \frac{\boldsymbol{\rho}_{i-1,j}^{n+1} + \boldsymbol{\rho}_{i-1,j}^{n}}{2} - b_{i+1,j}^{n+1/2} \frac{\boldsymbol{\rho}_{i+1,j}^{n+1} + \boldsymbol{\rho}_{i+1,j}^{n}}{2} \\ &- c_{i,j-1}^{n+1/2} \frac{\boldsymbol{\rho}_{i,j-1}^{n+1} + \boldsymbol{\rho}_{i,j-1}^{n}}{2} - d_{i,j+1}^{n+1/2} \frac{\boldsymbol{\rho}_{i,j+1}^{n+1} + \boldsymbol{\rho}_{i,j+1}^{n}}{2} \\ &= \mathcal{S}_{i,j} \mathbf{C}(\boldsymbol{\rho}_{i,j}^{n+1}, \mathbf{R}_{i,j}^{n+1/2}) \boldsymbol{\rho}_{i,j}^{n+1}. \end{aligned} \tag{20}$$

Notice that the non linear system (20) has the same structure of (14) so that we can use the procedure of Remark 11 to solve it. Analogous schemes result for vibrational energies. Momenta and total energy result in the following scheme:

$$\frac{\mathcal{S}_{i,j}}{\Delta t}(\mathbf{X}_{i,j}^{n+1}-\mathbf{X}_{i,j}^{n})+e_{i,j}^{n}\frac{\mathbf{X}_{i,j}^{n+1}+\mathbf{X}_{i,j}^{n}}{2}$$
$$-a_{i-1,j}^{n+1/2}\frac{\mathbf{X}_{i-1,j}^{n+1}+\mathbf{X}_{i-1,j}^{n}}{2}-b_{i+1,j}^{n+1/2}\frac{\mathbf{X}_{i+1,j}^{n+1}+\mathbf{X}_{i+1,j}^{n}}{2}$$
$$-c_{i,j-1}^{n+1/2}\frac{\mathbf{X}_{i,j-1}^{n+1}+\mathbf{X}_{i,j-1}^{n}}{2}-d_{i,j+1}^{n+1/2}\frac{\mathbf{X}_{i,j+1}^{n+1}+\mathbf{X}_{i,j+1}^{n}}{2}=-\mathbf{r}_{i,j}$$

where

$$\mathbf{r}_{i,j}=\mathbf{f}_{i+1/2,j}-\mathbf{f}_{i-1/2,j}+\mathbf{f}_{i,j+1/2}-\mathbf{f}_{i,j-1/2},$$

$$\mathbf{f}_{i+1/2,j}=\rho_{i,j}^{n+1/2}\mathbf{a}_{i,j}^{n+1/2}-\rho_{i+1,j}^{n+1/2}\mathbf{b}_{i+1,j}^{n+1/2},\qquad \mathbf{f}_{i,j+1/2}=\rho_{i,j}^{n+1/2}\mathbf{c}_{i,j}^{n+1/2}-\rho_{i,j+1}^{n+1/2}\mathbf{d}_{i,j+1}^{n+1/2},$$

and

$$\mathbf{a}_{i,j}^{n+1/2}=\ell_{i+1/2,j}\left(\mathbf{a}_1(\mathbf{U}_{i,j}^{n+1/2},\mathbf{n}_{i+1/2,j})\begin{bmatrix}(n_x)_{i+1/2,j}\\(n_y)_{i+1/2,j}\\\mathbf{v}_{i,j}\cdot\mathbf{n}_{i+1/2,j}\end{bmatrix}+\mathbf{a}_2(\mathbf{U}_{i,j}^{n+1/2},\mathbf{n}_{i+1/2,j})\begin{bmatrix}0\\0\\1\end{bmatrix}\right),$$

$$\mathbf{b}_{i,j}^{n+1/2}=\ell_{i-1/2,j}\left(\mathbf{a}_1(\mathbf{U}_{i,j}^{n+1/2},-\mathbf{n}_{i-1/2,j})\begin{bmatrix}(-n_x)_{i-1/2,j}\\(-n_y)_{i-1/2,j}\\-\mathbf{v}_{i,j}\cdot\mathbf{n}_{i-1/2,j}\end{bmatrix}+\mathbf{a}_2(\mathbf{U}_{i,j}^{n+1/2},-\mathbf{n}_{i-1/2,j})\begin{bmatrix}0\\0\\1\end{bmatrix}\right),$$

$$\mathbf{c}_{i,j}^{n+1/2}=\ell_{i,j+1/2}\left(\mathbf{a}_1(\mathbf{U}_{i,j}^{n+1/2},\mathbf{n}_{i,j+1/2})\begin{bmatrix}(n_x)_{i,j+1/2}\\(n_y)_{i,j+1/2}\\\mathbf{v}_{i,j}\cdot\mathbf{n}_{i,j+1/2}\end{bmatrix}+\mathbf{a}_2(\mathbf{U}_{i,j}^{n+1/2},\mathbf{n}_{i,j+1/2})\begin{bmatrix}0\\0\\1\end{bmatrix}\right),$$

$$\mathbf{d}_{i,j}^{n+1/2}=\ell_{i,j-1/2}\left(\mathbf{a}_1(\mathbf{U}_{i,j}^{n+1/2},-\mathbf{n}_{i,j-1/2})\begin{bmatrix}(-n_x)_{i,j-1/2}\\(-n_y)_{i,j-1/2}\\-\mathbf{v}_{i,j}\cdot\mathbf{n}_{i,j-1/2}\end{bmatrix}+\mathbf{a}_2(\mathbf{U}_{i,j}^{n+1/2},-\mathbf{n}_{i,j-1/2})\begin{bmatrix}0\\0\\1\end{bmatrix}\right),$$

Second order in space accuracy

The upwind flux (12) is only first order accurate in space. It is possible to improve the accuracy by some flux-limiter technique substituting the upwind flux (12) with the following:

$$\mathbf{F}(\mathbf{U},\mathbf{V},\mathbf{n})=\theta\left(\mathbf{F}^{+}(\mathbf{U},\mathbf{n})-\mathbf{F}^{+}(\mathbf{V},-\mathbf{n})\right)+\frac{1-\theta}{2}\left(\mathbf{F}(\mathbf{U},\mathbf{n})-\mathbf{F}(\mathbf{V},-\mathbf{n})\right),$$

where θ, for the present, is an unspecified parameter. Note that if $\theta = 0$ we obtain a second order flux, while with $\theta = 1$ we obtain the original first order flux. The scheme with $\theta = 0$ is unstable, however increasing (locally) the value of θ we can obtain a quasi second order scheme. The approach used here uses some ideas from the high resolution schemes extensively studied in the literature (Harten, 1983; 1984; 1987; Harten *et al.*, 1976; Rider, 1993; Saltzman, 1994; Shu, 1987; Swanson and Turkel, 1992; Sweby, 1984). Here we use a simpler approach based on an euristic limiter which does not use e.g. wave decomposition. To limit the value of θ we use the following procedure:

- For each cell (i, j) we calculate that the local CFL numbers in the horizontal and vertical direction $c^h_{i,j}$, $c^v_{i,j}$ as follows

$$c^h_{i,j} = \Delta t(|\,\mathbf{v}_{i,j} \cdot \mathbf{n}^h_{i,j}\,| + c)\frac{\max(\ell_{i+1/2,j}, \ell_{i-1/2,j})}{\mathcal{S}_{i,j}},$$

$$c^v_{i,j} = \Delta t(|\,\mathbf{v}_{i,j} \cdot \mathbf{n}^v_{i,j}\,| + c)\frac{\max(\ell_{ij+1/2,}, \ell_{i,j-1/2})}{\mathcal{S}_{i,j}},$$

where

$$\mathbf{n}^h_{i,j} = \frac{\mathbf{n}_{i+1/2,j} + \mathbf{n}_{i-1/2,j}}{2}, \qquad \mathbf{n}^v_{i,j} = \frac{\mathbf{n}_{i,j+1/2} + \mathbf{n}_{i,j-1/2}}{2}.$$

- For each cell (i, j) the ratios related with the local CFL numbers are evaluated

$$r^h_{i,j} = \left(\frac{\mathcal{S}_{i+1,j} + \mathcal{S}_{i,j}}{\mathcal{S}_{i,j} + \mathcal{S}_{i-1,j}}\right)\left(\frac{\ell_{i-1/2,j}}{\ell_{i+1/2,j}}\right)\left|\frac{c^h_{i+1,j} - c^h_{i,j}}{c^h_{i,j} - c^h_{i-1,j}}\right|,$$

$$r^v_{i,j} = \left(\frac{\mathcal{S}_{i,j+1} + \mathcal{S}_{i,j}}{\mathcal{S}_{i,j} + \mathcal{S}_{i,j-1}}\right)\left(\frac{\ell_{i,j-1/2}}{\ell_{i,j+1/2}}\right)\left|\frac{c^v_{i,j+1} - c^v_{i,j}}{c^v_{i,j} - c^v_{i,j-1}}\right|.$$

- At this point the θs associated to the edges are computed as follows

$$\theta_{i+1/2,j} = 1 - \min\left(r^h_{i,j}, 1/r^h_{i,j}, r^h_{i+1,j}, 1/r^h_{i+1,j}\right),$$

$$\theta_{i,j+1/2} = 1 - \min\left(r^v_{i,j}, 1/r^v_{i,j}, r^v_{i,j+1}, 1/r^v_{i,j+1}\right).$$

In the numerical procedure we have the edges fluxes split into two parts. The former is the upwind flux, the latter is the central flux. In the first half step the central fluxes are taken explicit, then into the second half step the central fluxes are evaluated at time step $n + 1/2$. The upwind fluxes are evaluated semi-implicitly as in the previous sections. In this way we have a minimal change in the solver because the contributions of the central fluxes are in the known term of linear and non-linear systems while the matrices, whose coefficient are multiplied by some θs, still remain M-matrices.

Numerical tests

One dimensional test cases

Sod test. The first test case is a classical one, the Sod test (Sod, 1978); it is a one dimensional test case, defined in the interval [0,1], with the following initial values

$$\text{(i) for } x < 0.5;\ \rho = 1\ Kg/m^3,\ u = 0\ m/s,\ p = 1\ Pa.$$

$$\text{(ii) for } x > 0.5;\ \rho = 0.125\ Kg/m^3,\ u = 0\ m/s,\ p = 0.1\ Pa.$$

The air is supposed composed of only N_2 so that $\gamma = 1 + \beta = 1.4$. Figures 3-6 show the solution at $t = 0.24s$. The solution was computed by using a fixed time step $\Delta t = 0.24s/50 = 0.0048s$ with a uniform grid of 100 cells.

Lax test. The second test case is another classical one, the Lax test (Lax, 1954); it is a one dimensional test case, defined in the interval [0,1], with the following initial values

$$\text{(i) for } x < 0.5;\ \rho = 0.445\ Kg/m^3,\ u = 0.698\ m/s,\ p = 3.528\ Pa.$$

$$\text{(ii) for } x > 0.5;\ \rho = 0.5\ Kg/m^3,\ u = 0\ m/s,\ p = 0.571\ Pa.$$

As in the previous test air is supposed composed of only N_2 so that $\gamma = 1 + \beta = 1.4$. Figures 7-10 show the solution at $t = 0.15s$. The solution was computed by using a fixed time step $\Delta t = 0.15s/60 = 0.0025s$ with an uniform grid of 100 cells.

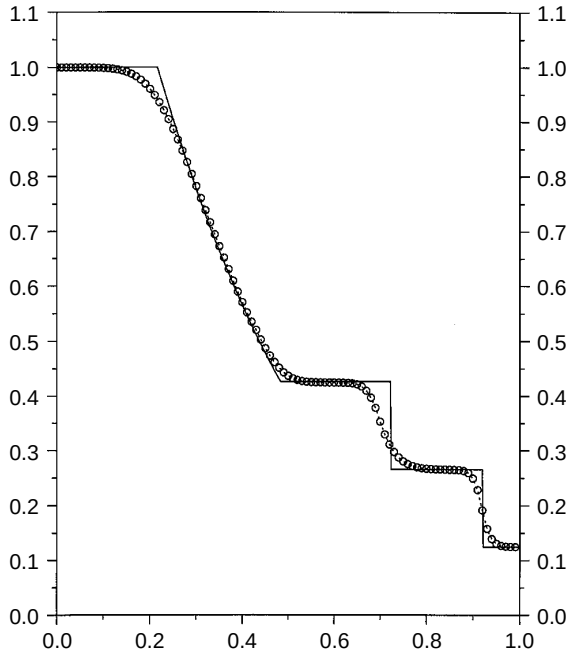

Figure 3.
Solution of Sod problem at time $t = 0.24s$; mass density distribution. The solid line is the exact solution

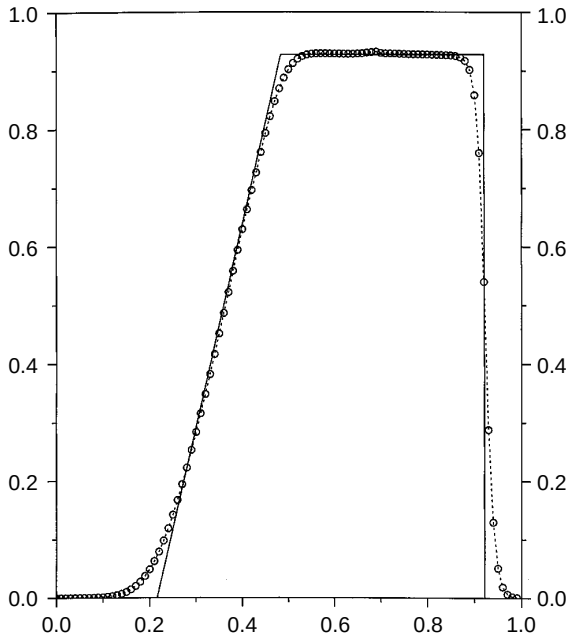

Figure 4.
Solution of Sod problem at time $t = 0.24s$; velocity distribution. The solid line is the exact solution

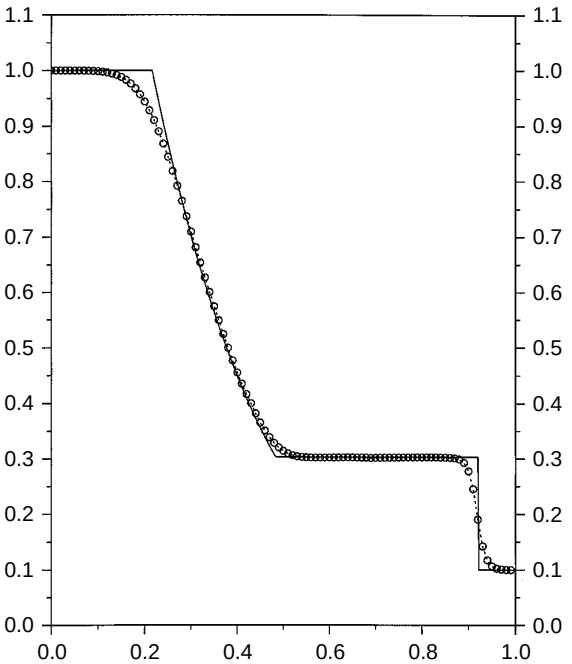

Figure 5.
Solution of Sod problem at time $t = 0.24s$; pressure distribution. The solid line is the exact solution

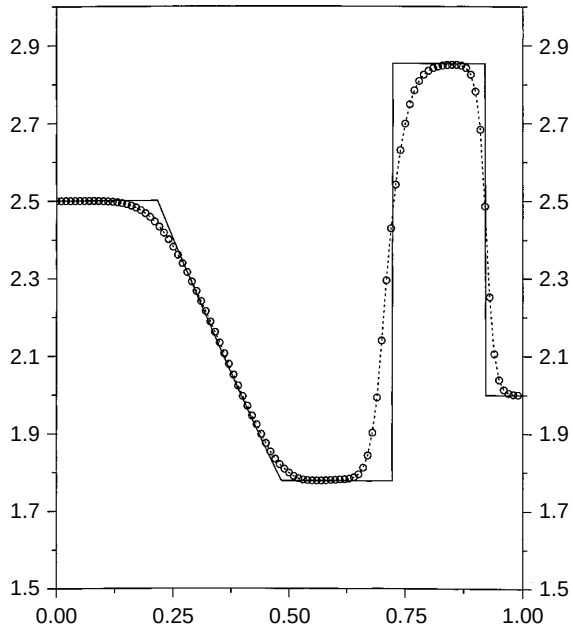

Figure 6. Solution of Sod problem at time $t = 0.24s$; internal energy $(E/\rho - u^2/2)$ distribution. The solid line is the exact solution

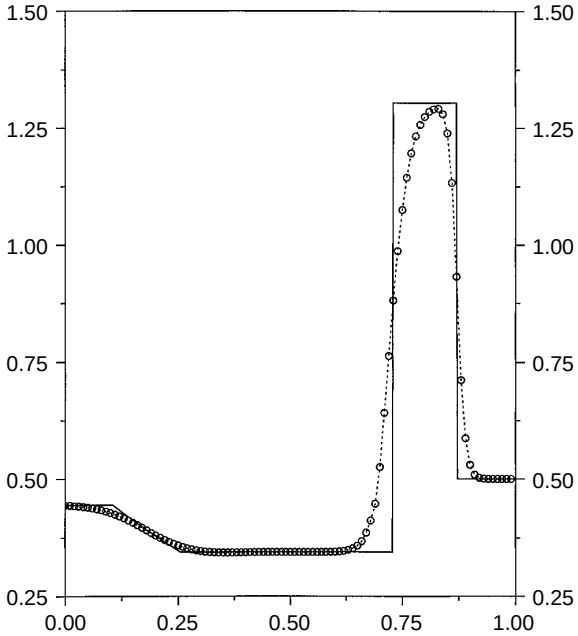

Figure 7. Solution of Lax problem at time $t = 0.15s$; mass density distribution. The solid line is the exact solution

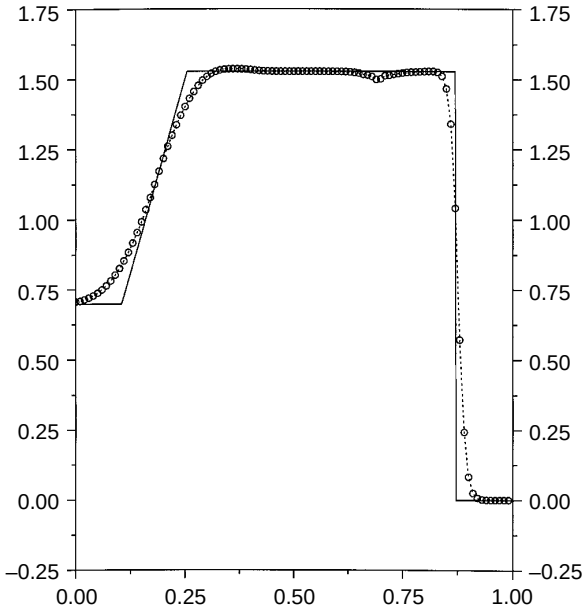

Figure 8.
Solution of Lax problem at time $t = 0.15s$; velocity distribution. The solid line is the exact solution

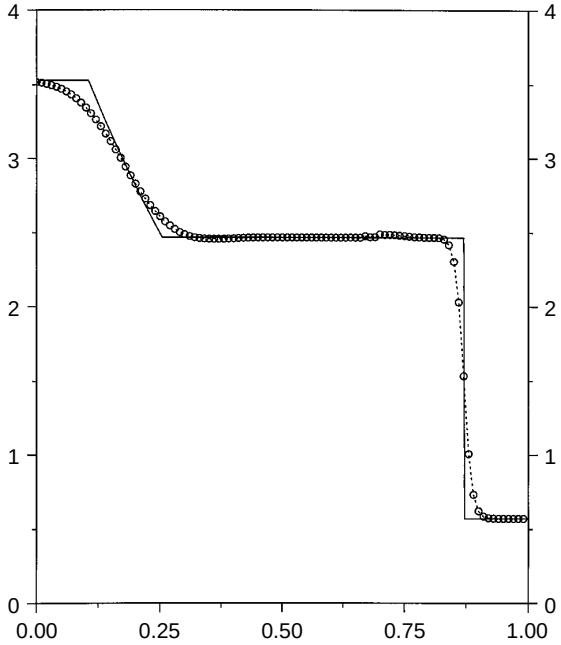

Figure 9.
Solution of Lax problem at time $t = 0.15s$; pressure distribution. The solid line is the exact solution

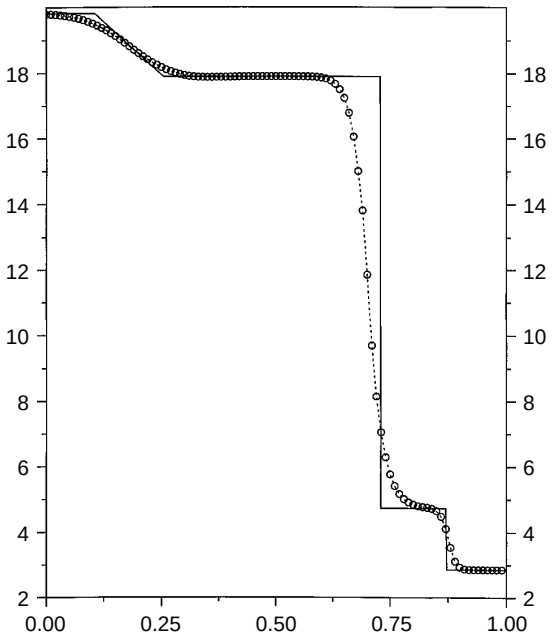

Figure 10. Solution of Lax problem at time $t = 0.15s$; internal energy $(E/\rho - u^2/2)$ distribution. The solid line is the exact solution

1D shock tube

The test case is defined as a one-dimensional tube with length $1m$ and with the following initial conditions:

(1) for $x < 0.5$; $T = 9{,}000K$, $\rho = 2.532Kg/m^3$, $u = 0m/s$.

(2) for $x > 0.5$; $T = 300K$, $\rho = 1.156Kg/m^3$, $u = 0m/s$.

In order to compare our results with those in Abgrall *et al.* (1992), instead of Dunn and Kang model (Dunn and Kang, 1973), the Park dissociation and recombination model (Park, 1985) is used. At $9{,}000K$ with $\rho = 2.532Kg/m^3$ the Park model gives approximately the mass distribution described in Table II.

Frozen case. In this case we test the solver without chemistry source terms. The solution is presented at time $t = 160\mu s$ and was computed by using a fixed time step $\Delta t = 160\mu s/60 = 2.\bar{6}\mu s$ with an uniform grid of 100 cells. The results are compared with those in Abgrall *et al.* (1992) (which use a grid of 101 points). We can see that the proposed code is slightly more diffusive than that in Abgrall *et al.* (1992) but the agreement is good. In Figure 11 one can see mass fraction distributions. In Figures 12-15 we have displayed the density, velocity, pressure and temperature.

$T(K)$	$\rho(Kg/m^3)$	$N_2(\%)$	$O_2(\%)$	$NO(\%)$	$N(\%)$	$O(\%)$
9,000	2.532	44.2	7.36×10^{-2}	2.3	31.4	22
300	1.156	76.7	23.3	0	0	0

Table II.

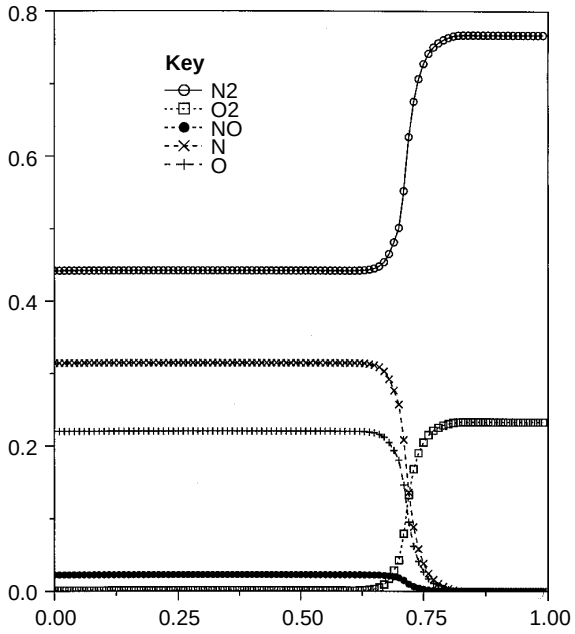

Figure 11.
Solution of Shock Tube problem at time $t = 160\mu s$; mass fraction distributions. Non-reactive case

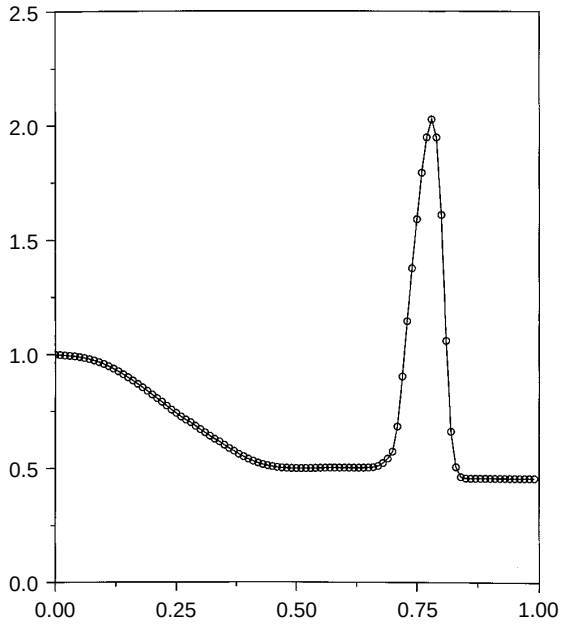

Figure 12.
Solution of Shock Tube problem at time $t = 160\mu s$; scaled mass density distribution. Non-reactive case

Test with chemistry source terms. The solution is presented at time $t = 160\mu s$ and was computed by using a fixed time step $\Delta t = 160\mu s/120 = 1.\bar{3}\mu s$ with a uniform grid of 200 cells. The results are compared with those in Abgrall *et al.*

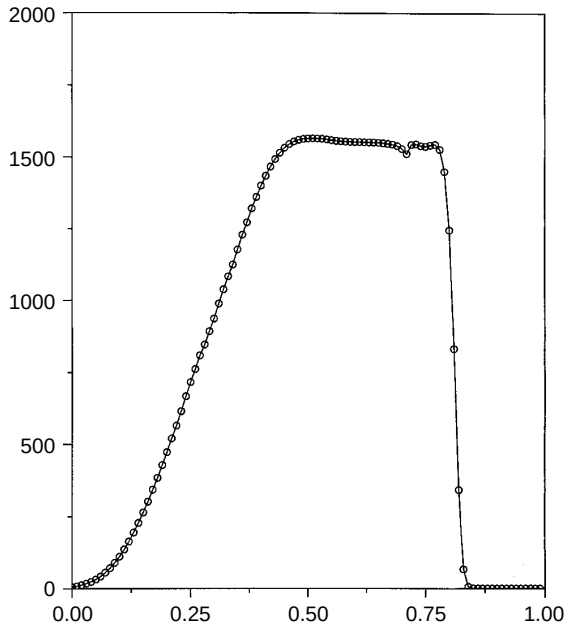

Figure 13.
Solution of Shock Tube problem at time $t = 160\mu s$; velocity distribution. Non-reactive case

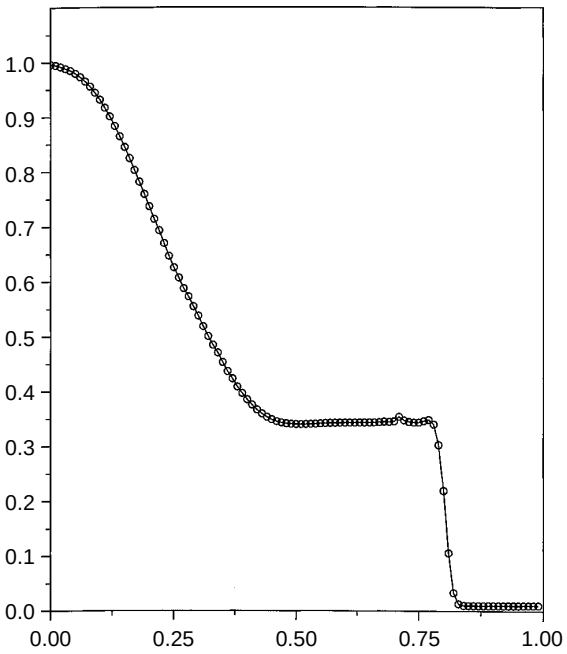

Figure 14.
Solution of Shock Tube problem at time $t = 160\mu s$; scaled pressure distributions. Non-reactive case

(1992) (which use a grid of 201 points). A comparison of the computed results with those in Abgrall *et al.* (1992) shows that the agreement is good except for the velocity that is more smeared. In Figure 16 we can see mass fractions

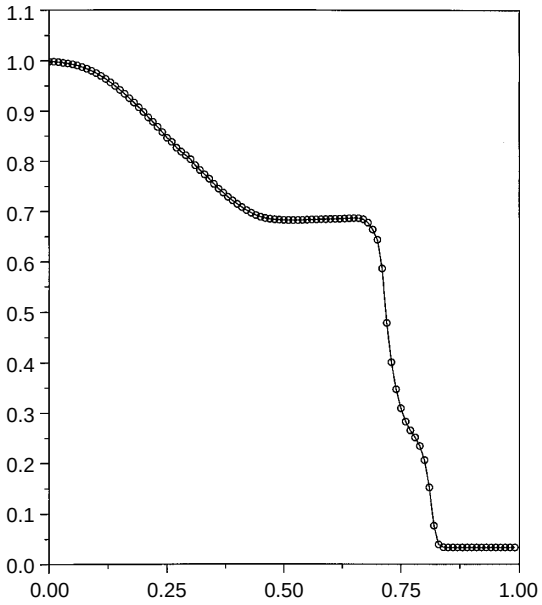

Figure 15.
Solution of Shock Tube problem at time $t = 160\mu s$; scaled temperature distribution. Non-reactive case

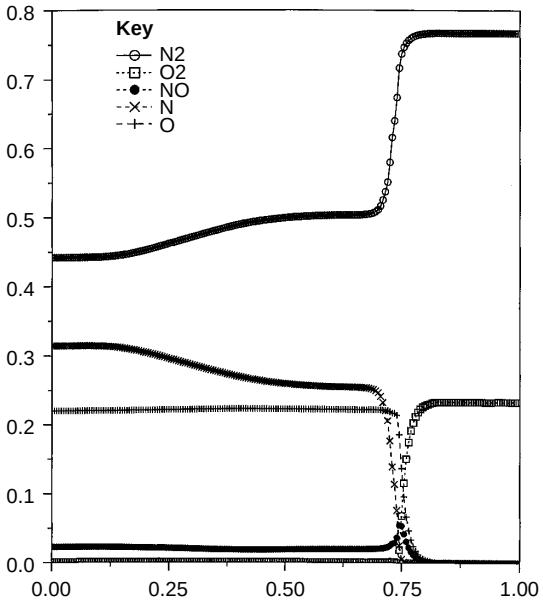

Figure 16.
Solution of Shock Tube problem at time $t = 160\mu s$; mass fraction distributions. Non-reactive case

distributions, in Figure 18, mass density distribution and in Figure 21, temperature distribution. In Figure 17 we can note the production of *NO* at the contact discontinuity, this can explains the small wiggles in the velocity and pressure (Figures 19-20) as in Abgrall *et al.* (1992).

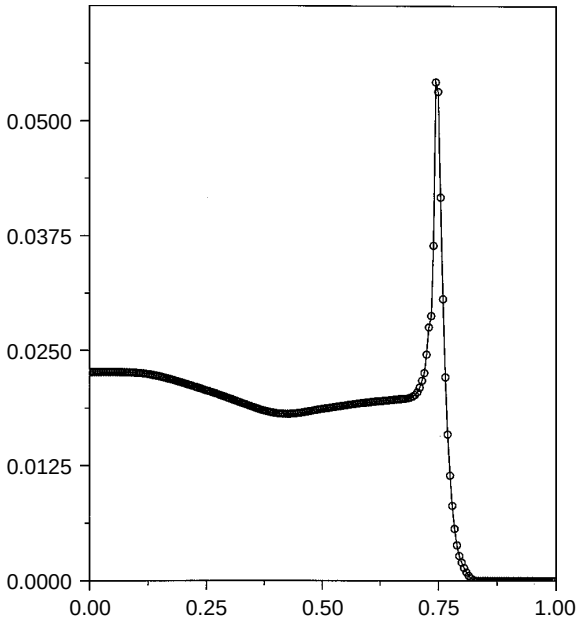

Figure 17.
Solution of Shock Tube problem at time $t = 160\mu s$; NO mass fraction distribution. Reactive case

Two dimensional test cases

The 2D test cases are taken from Groth and Gottlieb (1993). The problems considered are the following: the single, complex and double Mach reflections in

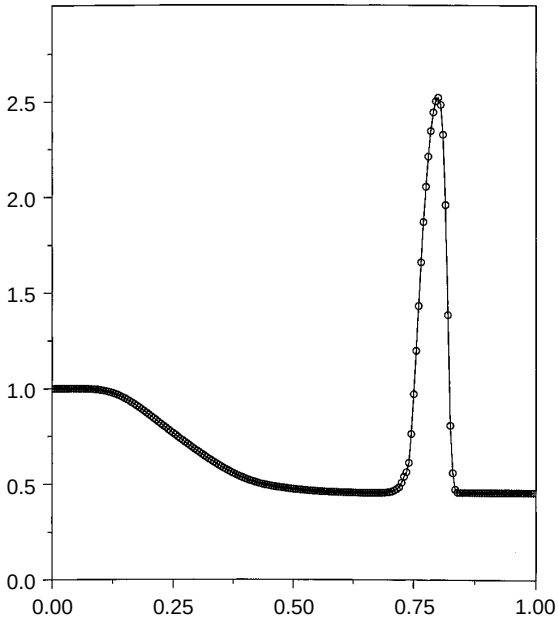

Figure 18.
Solution of Shock Tube problem at time $t = 160\mu s$; scaled mass density distribution. Reactive case

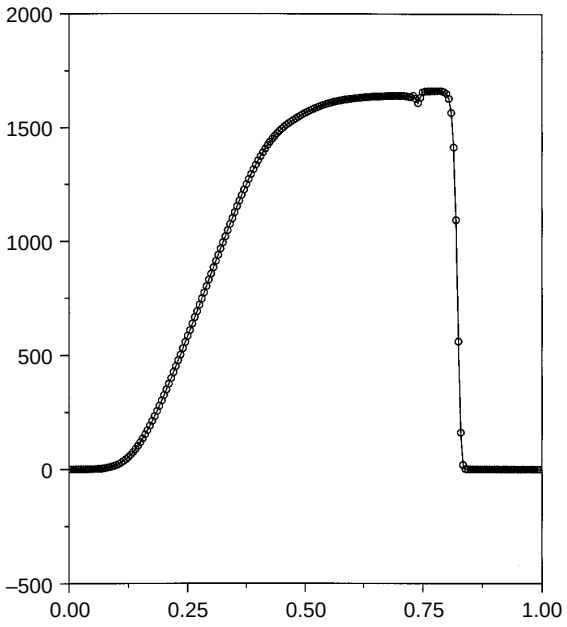

Figure 19.
Solution of Shock Tube problem at time $t = 160\mu s$; velocity distribution. Reactive case

air of a planar incident shock from a wedge; the diffraction of a planar high-Mach-number incident shock at an expansion corner in oxygen; the blunt-body flow in nitrogen. Except for the last, they are all non-stationary flow problems

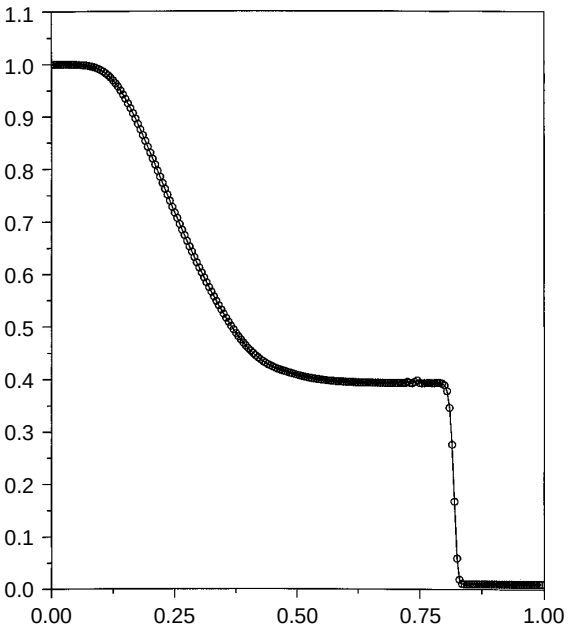

Figure 20.
Solution of Shock Tube problem at time $t = 160\mu s$; scaled pressure distribution. Reactive case

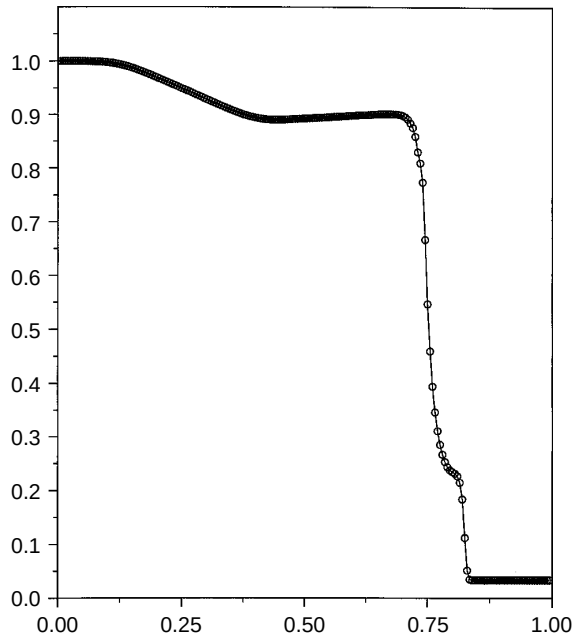

Figure 21.
Solution of Shock Tube problem at time $t = 160\mu s$; scaled temperature distribution. Reactive case

and use the Dunn and Kang dissociation and recombination model for the source terms.

Single Mach reflection in air

This test case is the oblique reflection of a $M_s = 2.03$ planar shock wave propagating in air incident on a 27^0 compression corner. The value of the temperature and density of the quiescent air ahead of the shock are $299.2K$ and $0.387Kg/m^3$. The mass fraction of the quiescent air is assumed to be composed of 76.7 per cent of N_2 and 23.3 per cent of O_2. The value of pressure, temperature and density of the supersonic inlet were specified by solving the Rankine-Hugoniot conditions. In this test case non-equilibrium effects are insignificant. So it is a test for the capabilities of the gas-dynamic solver. The solution is presented at time $t = 100\mu s$ and was computed by using a fixed time step $\Delta t = 100\mu s/300 = 0.\bar{3}\mu s$ with a 300×100 node mesh. Figure 22 depicts the density contour while Figure 23 depicts the wall density distributions. The results are in good agreement with those in Groth and Gottlieb (1993).

Complex Mach reflection in air

This test case is the oblique reflection of a $M_s + 10.37$ planar shock wave propagating in air incident on a 10^0 compression corner. The value of the temperature and density of the quiescent air ahead of the shock are $299K$ and $0.0777Kg/m^3$, respectively. The mass fraction of the quiescent air is assumed to be composed of 76.7 per cent of N_2 and 23.3 per cent of O_2. The value of

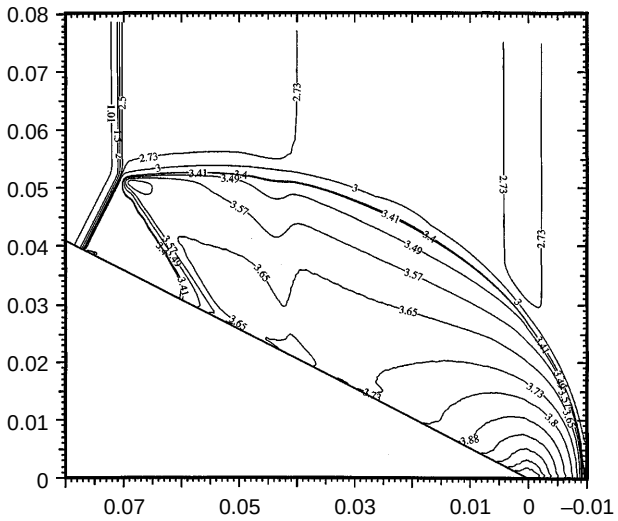

Figure 22.
Single Mach reflection in air; mass density ratio (ρ/ρ_0) distribution, where ρ_0 is the density of quiescent air. Axes units are in metres

pressure, temperature and density of the supersonic inlet were specified by solving the Rankine-Hugoniot conditions. The solution is presented at time $t = 20\mu s$ and was computed by using a fixed time step $\Delta t = 20\mu s/600 = 0.0\bar{3}\mu s$ with a 450×125 node mesh. Figures 24 and 25 depict respectively the density contour and the wall density distributions. The results are in good agreement with those in Groth and Gottlieb (1993).

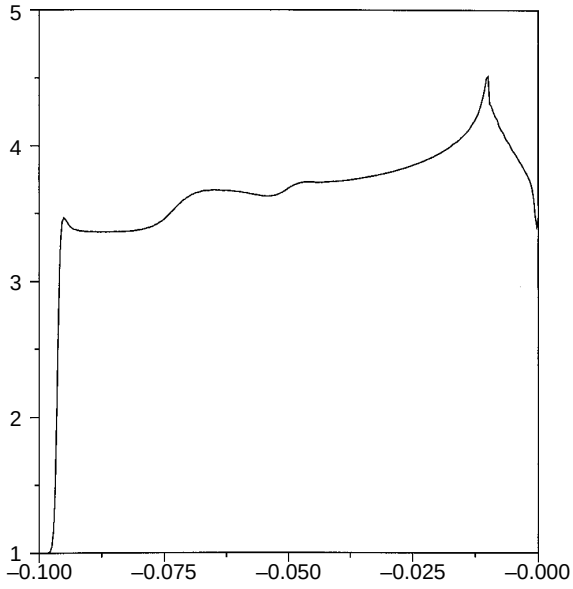

Figure 23.
Single Mach reflection in air; wall mass density distribution

Double Mach reflection in air

This test case is the oblique reflection of a $M_s = 8.7$ planar shock wave propagating in air incident on a 27^0 compression corner. The value of the temperature and density of the quiescent air ahead of the shock are $299.2K$ and $0.0476Kg/m^3$, respectively. The mass fraction of the quiescent air is assumed to be composed of 76.7 per cent of N_2 and 23.3 per cent of O_2. The value of pressure, temperature and density of the supersonic inlet were specified by solving the Rankine-Hugoniot conditions. The solution is presented at time $t = 22\mu s$ and was computed by using a fixed time step $\Delta t = 22\mu s/700 \approx 0.0314\mu s$ with a 500×100 node mesh. Figures 26 and 27 depict respectively the density contour and the wall density distributions. The results are in good agreement with those in Groth and Gottlieb (1993).

Shock wave diffraction in oxygen

This test case is the prediction of the non-stationary planar flow of a $M_s = 12$ planar shock wave of dissociated oxygen around a 15^0 expansion corner. The value of the temperature and density of the quiescent air ahead of the shock are $300K$ and $0.0342Kg/m^3$. The post-shock state of the oxygen is approximately 23 per cent dissociated. The value of pressure, temperature and density of the supersonic inlet were specified by solving the Rankine-Hugoniot conditions. The solution is presented at time $t = 21.7\mu s$ after the shock travel the corner and was computed by using a fixed time step $\Delta t = 21.7\mu s/420 \approx 0.0512\mu s$ with a 250×100 node mesh. Figure 28 depicts the density contour. The results are in good agreement with those in Groth and Gottlieb (1993).

Blunt-body flow in nitrogen

This test case is the prediction of the stationary planar flow of pure nitrogen around a two-dimensional circular cylinder with axis of symmetry perpendicular to the free-stream flow directions. The radius of the cylinder is $2.54cm$ while the free-stream density ρ_∞, temperature T_∞ and velocity u_∞ are $0.0055Kg/m^3$, $1400K$ and $5500m/s$, respectively. The solution was computed by using a $100 \times$

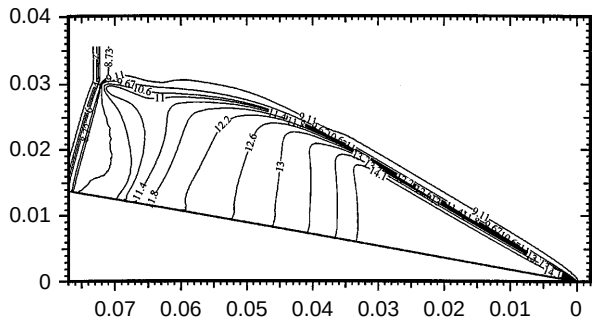

Figure 24. Complex mach reflection in air; mass density ratio (ρ/ρ_0) distribution, where ρ_0 is the density of quiescent air. Axes units are in metres

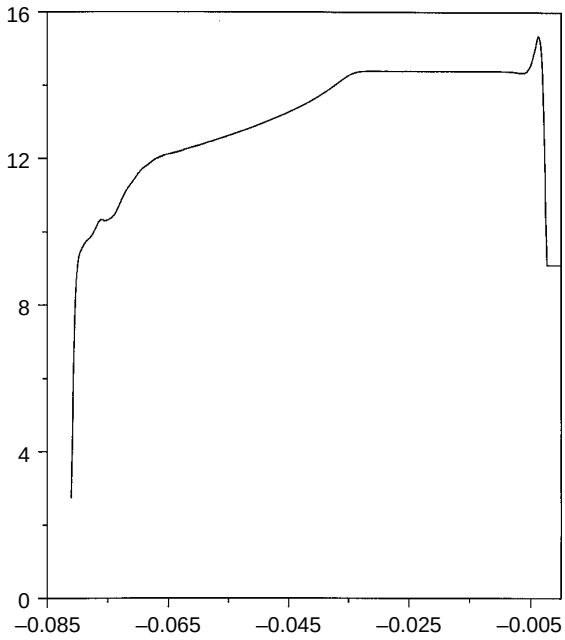

Figure 25.
Complex Mach reflection in air; wall mass density distribution

100 node mesh. Figure 29 depicts the density contour. The results are in good agreement with those in Groth and Gottlieb (1993).

The iterative procedure for the solution of the non linear system for the densities is described in Remark 11. Similar schemes are used for the solution of the linear system for vibrational energies and velocities-energy. The residual r = **b** – **A**x is scaled component by component by the diagonal of **A** as follows:

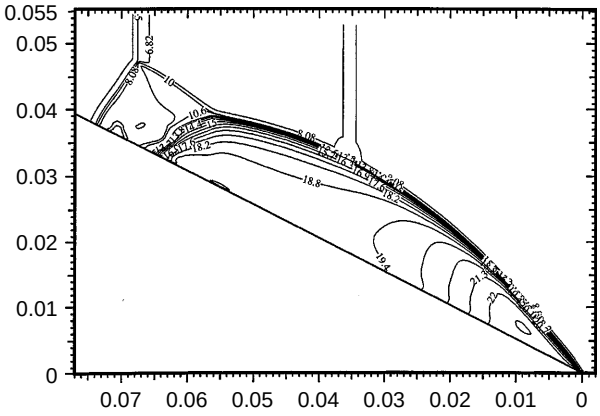

Figure 26.
Double Mach reflection in air; mass density ratio (ρ/ρ_0) distribution, where ρ_0 is the density of quiescent air. Axes units are in metres

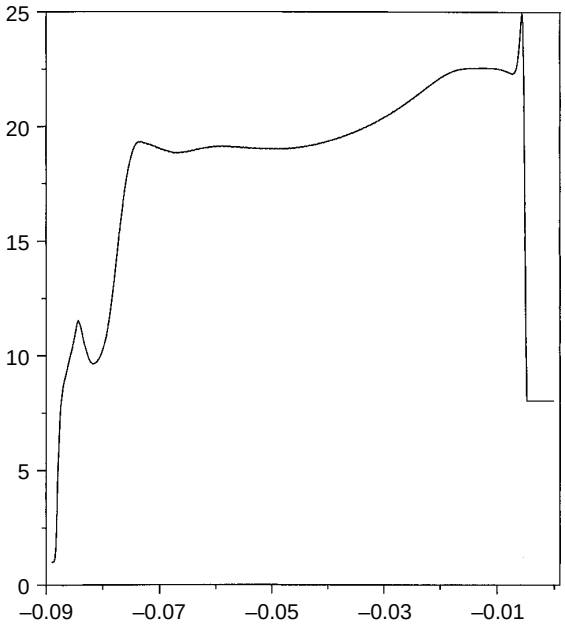

Figure 27.
Single mass reflection in air; wall mass density distribution

$$\frac{|r_i|}{|A_{i,i}|}$$

The iterations are stopped if the scaled residual is less than 10^{-6}. To speed up the solution procedure for the densities, the system is solved at first assuming no-chemistry present, and then this solution is used as the starting point for the complete iterative procedure. Table III is a summary of the computational costs of the scheme in terms of the average number of iteration per time step. This table contains only the average values of the second half step so that, in practice, the average total cost per time step is about twice the value in the table.

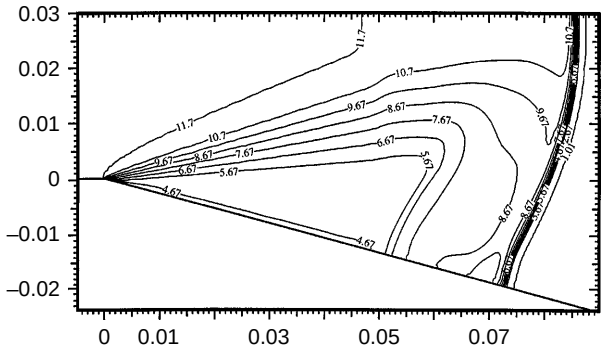

Figure 28.
Shock wave diffraction in oxygen; mass density ratio (ρ/ρ_0) distribution, where ρ_0 is the density of quiescent air. Axes units are in metres

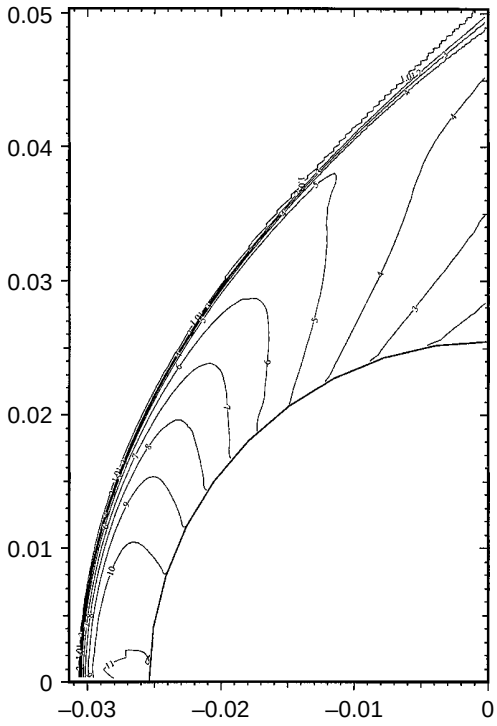

Figure 29.
Blunt-body flow in nitrogen; mass density ratio (ρ/ρ_∞) distribution, where $\rho_\infty = 5500 kg/m^3$. Axes units are in metres

Test case	NoChem	Chem	EV	UV	E
Single Mach	4	0	4.018	5.037	4.013
Complex Mach	4	5.992	5	5.008	4.998
Double Mach	4	5.966	5	5.004	4.349
Diffraction	4	3.998	5.027	5	4.027

Notes: NoChem = iteration for density without activated chemistry, Chem = iteration for density with activated chemistry, EV = iteration for vibrational energies, UV = iterations for velocity system, E = iterations for total energy system

Table III.
Average iterations

Conclusions

The present finite volume scheme allows numerical solutions of hypersonic flows to be obtained at a relatively low computational cost. Positivity of the densities and vibrational energies is assured, for the first order scheme, even when large time steps are used. The method is quite general and can be extended to three dimensional problems, where the reduction of the computational cost is essential.

Appendix

We prove here the theorems stated in the paper. We denote by $\mathbb{R}_+$ and $\mathbb{R}^n_+$ the following subsets of $\mathbb{R}$ and $\mathbb{R}^n$

$$\mathbb{R}_+ = \{x \in \mathbb{R} \mid x \geq 0\}, \qquad \mathbb{R}^n_+ = \underbrace{\mathbb{R}_+ \times \mathbb{R}_+ \times \cdots \times \mathbb{R}_+}_{n-times}$$

Lemma 1. Let $\mathbf{v} \in \mathbb{R}^n$ be such that $\sum_{i=1}^n v_i = 0$ and let f: $\mathbb{R}^n_+ \mapsto \mathbb{R}_+$ be a continuous function, such that, for those k which satisfy $v_k < 0$, $f(\mathbf{x})/x_k$ is also continuous on $\mathbb{R}^n_+$.

Then $f(\mathbf{x})\mathbf{v}$ can be written as $\mathbf{C}(\mathbf{x})\mathbf{x} = f(\mathbf{x})\mathbf{v}$, where $\mathbf{C}(\mathbf{x})$ is a matrix with continuous entries such that

$$\begin{aligned} &C_{i,i}(\mathbf{x}) \leq 0, && i = 1, 2, \ldots, n \\ &C_{i,j}(\mathbf{x}) \geq 0, && i \neq j \\ &\sum_{i=1}^{n} C_{i,j}(\mathbf{x}) = 0, && j = 1, 2, \ldots, n \end{aligned} \tag{21}$$

Proof

Let $\mathbf{v} = \mathbf{v}^+ + \mathbf{v}^-$ where

$$\begin{aligned} \mathbf{v}^+ &= [\max(0, v_1), \max(0, v_2), \ldots, \max(0, v_n)]^T, \\ \mathbf{v}^- &= [\min(0, v_1), \min(0, v_2), \ldots, \min(0, v_n)]^T. \end{aligned} \tag{22}$$

By (22), it is possible to define the matrix $\mathbf{C}(\mathbf{x})$

$$\mathbf{C}(\mathbf{x}) = \sum_{i=1}^{n} \left(\frac{f(\mathbf{x})}{x_i} v_i^- \right) \left[\mathbf{e}_i - \frac{\mathbf{v}^+}{\| \mathbf{v}^+ \|_1} \right] \mathbf{e}_i^T,$$

where e_j are the vector of the canonical base in $\mathbb{R}^n$, i.e. $\mathbf{e}_j = [0, \ldots, 0, 1, 0, \ldots, 0]^T$. By a straightforward computation it is easy to verify that (21) holds.

Theorem 1. The source terms $\mathbf{W}(\rho, \mathbf{R})$ can be written in the form $\mathbf{C}(\rho, \mathbf{R})\rho$, where $\mathbf{C}(\rho, \mathbf{R})$ is a 5×5 matrix with continuous entries, such that:

(a) $C_{i,i}(\rho, \mathbf{R}) \leq 0 \qquad i = 1, 2, 3, 4, 5$

(b) $C_{i,j}(\rho, \mathbf{R}) \leq 0 \qquad i \neq j$

(c) $\sum_{i=1}^{5} C_{i,j}(\rho, \mathbf{R}) = 0 \qquad j = 1, 2, 3, 4, 5$

Proof

The source terms $\mathbf{W}(\rho, \mathbf{R})$ can be written as

$$\mathbf{W}(\rho, \mathbf{R}) = \sum_{j=1}^{10} f_j(\rho, \mathbf{R}) \mathbf{v}_j,$$

where we have set

$$\mathbf{v}_{j+5} = -\mathbf{v}_j, \qquad f_{j+5} = b_j, \qquad j = 1, 2, 3, 4, 5$$

For each fixed value of $\mathbf{R}$, the pair f_j, $\mathbf{v}_j$ satisfies the hypothesis of Lemma 1, so that we can state that

$$\mathbf{C}^{(j)}(\boldsymbol{\rho},\mathbf{R})\boldsymbol{\rho} = f_j(\boldsymbol{\rho},\mathbf{R})\mathbf{v}_j, \qquad j = 1,2,\ldots,10$$

with $\mathbf{C}^{(j)}(\rho, \mathbf{R})$ that satisfies the properties (a)-(c). Then it is possible to define

$$\mathbf{C}(\boldsymbol{\rho},\mathbf{R}) = \sum_{j=1}^{10} \mathbf{C}^{(j)}(\boldsymbol{\rho},\mathbf{R}),$$

and $\mathbf{C}(\rho, \mathbf{R})$ has obviously the properties (a)-(c).

Theorem 2 For each $i = 1, 2, \ldots, N_x$ and $j = 1, 2, \ldots, N_y$, let $\mathbf{C}^{(i,j)}$ be a matrix such that

$$\begin{aligned} &C^{(i,j)}_{k,k} \le 0, && k = 1,2,\ldots,N_z \\ &C^{(i,j)}_{k,l} \ge 0, && k \ne l \\ &\sum_{k=1}^{N_z} C^{(i,j)}_{k,l} \ge 0, && l = 1,2,\ldots,N_z \end{aligned} \tag{23}$$

for each i, j, let $\delta_{i,j}$, $\alpha_{i,j}$, $\beta_{i,j}$, $\gamma_{i,j}$, $\omega_{i,j} \in \mathbb{R}^+$ with $\delta_{i,j} > 0$. For each i, j, let $\mathbf{x}_{i,j}$, $\mathbf{z}_{i,j} \in \mathbb{R}^{N_z}$ and consider the linear system in the vector unknown $\mathbf{x}_{i,j}$, defined by the stencil

$$-\mathbf{C}^{(i,j)}\mathbf{x}_{i,j} + \begin{pmatrix} & -\omega_{i,j+1} & \\ -\alpha_{i-1,j} & \delta_{i,j} + \alpha_{i,j} + \beta_{i,j} + \gamma_{i,j} + \omega_{i,j} & -\beta_{i+1,j} \\ & -\gamma_{i,j-1} & \end{pmatrix} \mathbf{x}_{i,j} = \mathbf{b}_{i,j}, \tag{24}$$

with $i = 1, 2, \ldots, N_x$ and $j = 1, 2, \ldots, N_y$. The matrix of coefficients is an M-matrix. Therefore, if $\mathbf{b}_{i,j} \ge 0$, then the solution $\mathbf{x}_{i,j}$ is such that $\mathbf{x}_{i,j} \ge 0$ for all i, j.

Proof
Observe that the matrix of the system defined by (24) has positive elements on the main diagonal and non-positive elsewhere. The properties (23) imply that this matrix is strictly diagonal dominant, so that it is an M-matrix. By definition, this implies that $\mathbf{x}_{i,j} \ge 0$.

Corollary 1. The quantities x^{s+1} defined the iterative procedure of Table I are non-negative for all s

Proof
We apply theorem 2 with

$$\alpha_{i,j} = a_{i,j}, \quad \beta_{i,j} = b_{i,j}, \quad \gamma_{i,j} = c_{i,j}, \quad \omega_{i,j} = d_{i,j}, \quad \mathbf{C}^{(i,j)} = \mathcal{S}_{i,j}\mathbf{C}(\boldsymbol{\rho}_{i,j}, \mathbf{R}^n_{i,j}),$$

and

$$\delta_{i,j} = \frac{\mathcal{S}_{i,j}}{\Delta t} + \gamma_{i,j}, \quad \mathbf{z}_{i,j} = \left[\frac{\mathcal{S}_{i,j}}{\Delta t} + \gamma_{i,j}\right]\mathbf{x}^s_{i,j} + \frac{\mathcal{S}_{i,j}}{\Delta t}\boldsymbol{\rho}^n_{i,j} + \mathrm{bc}_{i,j}.$$

Corollary 2. The scheme in equation (18) maintains the vibrational energies non-negative.

Proof
we apply the theorem with

$$\alpha_{i,j} = a_{i,j}, \quad \beta_{i,j} = b_{i,j}, \quad \gamma_{i,j} = c_{i,j}, \quad \omega_{i,j} = d_{i,j}, \quad \mathbf{C}^{(i,j)} = 0,$$

and

$$\delta_{i,j} = \frac{\mathcal{S}_{i,j}}{\Delta t} + \frac{1}{(\tau_k)^n_{i,j}} - \frac{(\hat{W}_k^-)_{i,j}}{(\rho_k)^{n+1}_{i,j}},$$

$$\mathbf{z}_{i,j} = \mathcal{S}_{i,j}\left[\frac{1}{\Delta t} + \frac{1}{(\tau_k)^n_{i,j}} + \frac{(\hat{W}_k^+)_{i,j}}{(\rho_k)^{n+1}_{i,j}}\right](\mathcal{E}\mathrm{eq}_k)^n_{i,j} + \mathrm{bc}_{i,j}.$$

Theorem 3. The solutions of system (15) conserve the total amount of nitrogen and oxygen.

Proof

At the convergence the source term is

$$\hat{W}_{i,j} = \mathbf{C}(\boldsymbol{\rho}^{n+1}_{i,j}, \mathbf{R}^n_{i,j})\boldsymbol{\rho}^{n+1}_{i,j}. \tag{25}$$

By direct computation one can see that

$$(\hat{W}_1)_{i,j} + \alpha(\hat{W}_3)_{i,j} + (\hat{W}_4)_{i,j} = 0, \qquad (\hat{W}_2)_{i,j} + (1-\alpha)(\hat{W}_3)_{i,j} + (\hat{W}_5)_{i,j} = 0,$$

and also

$$\rho_N = \rho_1 + \alpha\rho_3 + \rho_4, \qquad \rho_O = \rho_2 + (1-\alpha)\rho_3 + \rho_5. \tag{26}$$

The following relations are also true

$$\begin{bmatrix} 1 \\ 0 \\ \alpha \\ 1 \\ 0 \end{bmatrix} \cdot \left(\mathbf{C}(\boldsymbol{\rho}^{n+1}_{i,j}, \mathbf{R}^n_{i,j})\boldsymbol{\rho}^{n+1}_{i,j}\right) = 0, \qquad \begin{bmatrix} 0 \\ 1 \\ 1-\alpha \\ 0 \\ 1 \end{bmatrix} \cdot \left(\mathbf{C}(\boldsymbol{\rho}^{n+1}_{i,j}, \mathbf{R}^n_{i,j})\boldsymbol{\rho}^{n+1}_{i,j}\right) = 0.$$

By multiplying system (15) at the left by the vectors [1, 0, α, 1, 0], [0, 1, 1 – α, 0, 1], and by using (25-26) we obtain

$$\begin{pmatrix} & -d_{i,j+1} & \\ -a_{i-1,j} & \frac{\mathcal{S}_{i,j}}{\Delta t} + e_{i,j} & -b_{i+1,j} \\ & -c_{i,j-1} & \end{pmatrix} x^{n+1}_{i,j} = \frac{\mathcal{S}_{i,j}}{\Delta t} x^n_{i,j}, \tag{27}$$

where $x = \rho_N, \rho_O$. Adding equations (27) over all the cells it follows now

$$\sum_{i,j} \frac{\mathcal{S}_{i,j}}{\Delta t} x^{n+1}_{i,j} = \sum_{i,j} \frac{\mathcal{S}_{i,j}}{\Delta t} x^n_{i,j} + \tag{28}$$

where the cancellation is due to the conservative form of (27). Equation (28) states that the variation of total quantity of nitrogen or oxygen depends only on the boundary terms, so that the possible changes are due only to the boundary conditions.

Theorem 4. For any n and fixed Δt there exists at least one non-negative solution of the non-linear system (15).

Proof

It will be sufficient to prove that the map Φ defined in Table I has a non-negative fixed point. For simplicity, we consider the map with $\Gamma_{i,j} = 0$. From Corollary 1 it follows that $\Phi(\mathbf{v}) \geq 0$ for all $\mathbf{v} \geq$

0. Denote by $\mathbf{x} = \Phi(\mathbf{v})$ the solution of the linear system of Table I. Introducing the vector $\mathbf{e} = [1, 1, 1, 1, 1]^T$, we can write

$$0 = \mathbf{e}^T \sum_{i,j=1}^{N_x,N_y} \Big\{ \mathbf{C}(v_{i,j}, \mathbf{R}_{i,j}^n)\mathbf{x}_{i,j} + e_{i,j}\mathbf{x}_{i,j} - a_{i-1,j}\mathbf{x}_{i-1,j} - b_{i+1,j}\mathbf{x}_{i+1,j} - c_{i,j-1}\mathbf{x}_{i,j-1} - d_{i,j+1}\mathbf{x}_{i,j+1} - \frac{\mathcal{S}_{i,j}}{\Delta t}\boldsymbol{\rho}_{i,j}^n \Big\}$$

$$= \sum_{i,j=1}^{N_x,N_y} \left\{ \left(\frac{\mathcal{S}_{i,j}}{\Delta t} + a_{i,j} + b_{i,j} + c_{i,j} + d_{i,j} \right) \| \mathbf{x}_{i,j} \|_1 - \frac{\mathcal{S}_{i,j}}{\Delta t} \| \boldsymbol{\rho}_{i,j}^n \|_1 \right\}$$

$$- \sum_{i,j=1}^{N_x,N_y} \{ a_{i-1,j} \| \mathbf{x}_{i-1,j} \|_1 + b_{i+1,j} \| \mathbf{x}_{i+1,j} \|_1 + c_{i,j-1} \| \mathbf{x}_{i,j-1} \|_1 + b_{i,j+1} \| \mathbf{x}_{i,j+1} \|_1 \} .$$

The dependence on $\mathbf{C}(v_{i,j}, \mathbf{R}_{i,j}^n)$ disappears because $\mathbf{e}^T\mathbf{C}(v_{i,j}, \mathbf{R}_{i,j}^n) = 0$ by condition (c) of Theorem 1. Next, we can write

$$0 = \sum_{j=1}^{N_y} \{ b_{1,j} \| \mathbf{x}_{1,j} \|_1 - a_{0,j} \| \mathbf{x}_{0,j} \|_1 - b_{N_x+1,j} \| \mathbf{x}_{N_x+1,j} \|_1 + a_{N_x,j} \| \mathbf{x}_{N_x,j} \|_1 \}$$

$$+ \sum_{i=1}^{N_x} \{ d_{i,1} \| \mathbf{x}_{i,1} \|_1 - c_{i,0} \| \mathbf{x}_{i,0} \|_1 - d_{i,N_y+1} \| \mathbf{x}_{i,N_y+1} \|_1 + c_{i,N_y} \| \mathbf{x}_{i,N_y} \|_1 \}$$

$$+ \sum_{i,j=1}^{N_x,N_y} \left\{ \frac{\mathcal{S}_{i,j}}{\Delta t} \| \mathbf{x}_{i,j} \|_1 - \frac{\mathcal{S}_{i,j}}{\Delta t} \| \boldsymbol{\rho}_{i,j}^n \|_1 \right\} .$$

Since $\mathbf{x}_{i,j}$ is known to be equal to $\rho_{i,j}^{n+1}$ at the boundary, it follows that

$$\sum_{j=1}^{N_y} \{ b_{1,j} \| \mathbf{x}_{1,j} \|_1 + a_{N_x,j} \| \mathbf{x}_{N_x,j} \|_1 \} + \sum_{i=1}^{N_x} \{ d_{i,1} \| \mathbf{x}_{i,1} \|_1 + c_{i,N_y} \| \mathbf{x}_{i,N_y} \|_1 \}$$

$$+ \sum_{i,j=1}^{N_x,N_y} \frac{\mathcal{S}_{i,j}}{\Delta t} \| \mathbf{x}_{i,j} \|_1 = \sum_{i,j=1}^{N_x,N_y} \frac{\mathcal{S}_{i,j}}{\Delta t} \| \boldsymbol{\rho}_{i,j}^n \|_1$$

$$+ \sum_{j=1}^{N_y} \{ a_{0,j} \| \boldsymbol{\rho}_{0,j}^{n+1} \|_1 + b_{N_x+1,j} \| \boldsymbol{\rho}_{N_x+1,j}^{n+1} \|_1 \} + \sum_{i=1}^{N_x} \{ c_{i,0} \| \boldsymbol{\rho}_{i,0}^{n+1} \|_1 + b_{i,N_y+1} \| \boldsymbol{\rho}_{i,N_y}^{n+1} \|_1 \} . \tag{29}$$

This suggest to define the norm

$$\| \mathbf{z} \| = \sum_{i,j=1}^{N_x,N_y} \frac{\mathcal{S}_{i,j}}{\Delta t} \| \mathbf{z}_{i,j} \|_1 + \sum_{j=1}^{N_y} \{ b_{1,j} \| \mathbf{z}_{1,j} \|_1 + a_{N_x,j} \| \mathbf{z}_{N_x,j} \|_1 \}$$

$$+ \sum_{i=1}^{N_x} \{ d_{i,1} \| \mathbf{z}_{i,1} \|_1 + c_{i,N_y} \| \mathbf{z}_{i,N_y} \|_1 \} .$$

By using this norm and in view of (29) one sees that $\| \Phi(\mathbf{v}) \| = K$, for all $\mathbf{v} \geq 0$ where

$$K = \sum_{i,j=1}^{N_x,N_y} \frac{\mathcal{S}_{i,j}}{\Delta t} \| \boldsymbol{\rho}_{i,j}^n \|_1 + \sum_{j=1}^{N_y} \{ a_{0,j} \| \boldsymbol{\rho}_{0,j}^{n+1} \|_1 + b_{N_x+1,j} \| \boldsymbol{\rho}_{N_x+1,j}^{n+1} \|_1 \}$$
$$+ \sum_{i=1}^{N_x} \{ c_{i,0} \| \boldsymbol{\rho}_{i,0}^{n+1} \|_1 + b_{i,N_y+1} \| \boldsymbol{\rho}_{i,N_y}^{n+1} \|_1 \} .$$

Introducing now the convex compact set

$$\mathcal{K} = \{ \mathbf{v} \geq 0 \,|\, \| \mathbf{v} \| = K \},$$

one sees that Φ is a continuous map from K into itself. By the Brouwer fixed point theorem (Zeidler, 1986), this map has at least one fixed point, that is a non-negative solution of the system (15)

Remark 14. Notice that the iteration map Φ can be written as:

$$\boldsymbol{\Phi}(\mathbf{v}) = \mathbf{x}, \qquad \text{where } \mathbf{x} \text{ is the solution of}$$

$$(\boldsymbol{\Gamma} + \mathbf{D}(\mathbf{v}) + \mathbf{M})\mathbf{x} = \boldsymbol{\Gamma}\mathbf{v} + \mathbf{b}, \quad \boldsymbol{\Gamma} = diag(\Gamma_{i,j}), \quad \mathbf{b}_{i,j} = \frac{\boldsymbol{\rho}_{i,j}^n \mathcal{S}_{i,j}}{\Delta t}.$$

Then, we can write

$$\boldsymbol{\Phi}(\mathbf{v}) = (\boldsymbol{\Gamma} + \mathbf{D}(\mathbf{v}) + \mathbf{M})^{-1}(\boldsymbol{\Gamma}\mathbf{v} + \mathbf{b}).$$

Also, in the proof of Corollary 1 we have seen that $\Gamma + \mathbf{D}(\mathbf{v}) + \mathbf{M}$ is an M-matrix, so that $(\Gamma + \mathbf{D}(\mathbf{v}) + \mathbf{M})^{-1} \geq 0$.

An estimate of the norm of the matrix $(\Gamma + \mathbf{D}(\mathbf{v}) + \mathbf{M})^{-1}$ is now obtained.

Lemma 2. It is $\| \mathbf{G}(\boldsymbol{\Gamma} + \mathbf{D}(\mathbf{v}) + \mathbf{M})^{-1} \|_1 \leq 1$, *where* $\mathbf{G} = diag\left(\Gamma_{i,j} + \frac{\mathcal{S}_{i,j}}{\Delta t} \right)$.

Proof

Let $\mathbf{e}$ be a vector with all components equal to 1. By a straightforward computation one has

$$\mathbf{e}^T(\boldsymbol{\Gamma} + \mathbf{D}(\mathbf{x}) + \mathbf{M}(\mathbf{x})) \geq \mathbf{e}^T\mathbf{G} \geq 0. \tag{30}$$

Multiplying now the equation (30) by $(\Gamma + \mathbf{D}(\mathbf{x}) + \mathbf{M}(\mathbf{x}))^{-1} \geq 0$, one has

$$\mathbf{e}^T = \mathbf{e}^T(\boldsymbol{\Gamma} + \mathbf{D}(\mathbf{x}) + \mathbf{M}(\mathbf{x}))(\boldsymbol{\Gamma} + \mathbf{D}(\mathbf{x}) + \mathbf{M}(\mathbf{x}))^{-1} \geq \mathbf{e}^T\mathbf{G}(\boldsymbol{\Gamma} + \mathbf{D}(\mathbf{x}) + \mathbf{M}(\mathbf{x}))^{-1} \geq 0. \tag{31}$$

From equation (31) it follows then $\| \mathbf{G}(\Gamma + \mathbf{D}(\mathbf{x}) + \mathbf{M}(\mathbf{x}))^{-1} \|_1 \leq 1$.

Corollary 3

$$\| (\boldsymbol{\Gamma} + \mathbf{D}(\mathbf{x}) + \mathbf{M}(\mathbf{x}))^{-1} \|_1 \leq \frac{1}{\| \mathbf{G} \|_1} \frac{\Delta t}{\min\limits_{i,j}^{N_x,N_y} (\Delta t \gamma_{i,j} + \mathcal{S}_{i,j})}.$$

Theorem 5 If Δt is small enough, then the map $\Phi : \mathsf{K} \mapsto \mathsf{K}$ is contractive

Proof

Take $x, y \in \mathsf{K}$ and let $\mathbf{N}(\mathbf{x}) = \Gamma + \mathbf{D}(\mathbf{x}) + \mathbf{M}$. Then

$$\begin{aligned}\boldsymbol{\Phi}(\mathbf{x}) - \boldsymbol{\Phi}(\mathbf{y}) &= \mathbf{N}(\mathbf{x})^{-1}(\boldsymbol{\Gamma}\mathbf{x} + \mathbf{b}) - \mathbf{N}(\mathbf{y})^{-1}(\boldsymbol{\Gamma}\mathbf{y} + \mathbf{b}),\\ &= \left[\mathbf{N}(\mathbf{x})^{-1} - \mathbf{N}(\mathbf{y})^{-1}\right]\mathbf{b} + \left[\mathbf{N}(\mathbf{x})^{-1}\boldsymbol{\Gamma}\mathbf{x} - \mathbf{N}(\mathbf{y})^{-1}\boldsymbol{\Gamma}\mathbf{y}\right],\\ &= \mathbf{N}(\mathbf{x})^{-1}\left[\mathbf{N}(\mathbf{y}) - \mathbf{N}(\mathbf{x})\right]\mathbf{N}(\mathbf{y})^{-1}\mathbf{b}\\ &+\mathbf{N}(\mathbf{x})^{-1}\boldsymbol{\Gamma}\left[\mathbf{x} - \mathbf{y}\right] + \mathbf{N}(\mathbf{x})^{-1}[\mathbf{N}(\mathbf{y}) - \mathbf{N}(\mathbf{x})]\mathbf{N}(\mathbf{y})^{-1}\boldsymbol{\Gamma}\mathbf{y}. \end{aligned} \tag{32}$$

Taking the $\|\cdot\|_1$ norm in (32), one then has

$$\begin{aligned}\|\boldsymbol{\Phi}(\mathbf{x}) - \boldsymbol{\Phi}(\mathbf{y})\|_1 \leq \|\mathbf{N}(\mathbf{x})^{-1}\|_1 \{\|\mathbf{N}(\mathbf{y})^{-1}\|_1 \|\mathbf{N}(\mathbf{y}) - \mathbf{N}(\mathbf{x})\|_1 [\|\mathbf{b}\|_1 + \|\boldsymbol{\Gamma}\mathbf{y}\|_1]\}\\ +\|\mathbf{N}(\mathbf{x})^{-1}\|_1 \|\mathbf{N}(\mathbf{y})^{-1}\|_1 \|\boldsymbol{\Gamma}\|_1 \|\mathbf{x} - \mathbf{y}\|_1. \end{aligned} \tag{33}$$

Observe that

$$\mathbf{N}(\mathbf{x}) - \mathbf{N}(\mathbf{y}) = (\boldsymbol{\Gamma} + \mathbf{D}(\mathbf{x}) + \mathbf{M}) - (\boldsymbol{\Gamma} + \mathbf{D}(\mathbf{y}) + \mathbf{M}) = \mathbf{D}(\mathbf{x}) - \mathbf{D}(\mathbf{y}),$$

and since $\mathbf{D}(\mathbf{z})$ is regular enough and does not depend on Δt, it is possible to find a constant L independent of Δt such that

$$\|\mathbf{M}(\mathbf{x}) - \mathbf{M}(\mathbf{y})\|_1 \leq \mathcal{L}\|\mathbf{x} - \mathbf{y}\|_1, \qquad \forall \mathbf{x}, \mathbf{y} \in \mathcal{K}.$$

Defining

$$g = \frac{\Delta t}{\min\limits_{i,j}^{N_x,N_y} (\Gamma_{i,j}\Delta t + \mathcal{S}_{i,j})},$$

from (33) one has

$$\begin{aligned}\|\boldsymbol{\Phi}(\mathbf{x}) - \boldsymbol{\Phi}(\mathbf{y})\|_1 &\leq g\{g\mathcal{L}[\|\mathbf{b}\|_1 + \|\boldsymbol{\Gamma}\mathbf{y}\|_1] + \|\boldsymbol{\Gamma}\|_1\}\|\mathbf{x} - \mathbf{y}\|_1,\\ &\leq g\left\{g\mathcal{L}\left[\|\mathbf{b}\|_1 + \max_{\mathbf{z}\in\mathcal{K}}\|\boldsymbol{\Gamma}\mathbf{z}\|_1\right] + \|\boldsymbol{\Gamma}\|_1\right\}\|\mathbf{x} - \mathbf{y}\|_1. \end{aligned}$$

Notice that for $\Delta t \mapsto 0$, we have $g\|\mathbf{b}\|$ bounded and $g \mapsto 0$. Consequently,

$$g\left\{g\mathcal{L}\left[\|\mathbf{b}\|_1 + \max_{\mathbf{z}\in\mathcal{K}}\|\boldsymbol{\Gamma}\mathbf{z}\|_1\right] + \|\boldsymbol{\Gamma}\|_1\right\} < 1,$$

for Δt small enough. Thus, the map $\Phi : \mathsf{K} \mapsto \mathsf{K}$ becomes contractive.

References and further reading

Abgrall, R., Fezoui, L. and Talandier, J. (1992), "An extension of Osher's Riemann solver for chemical and vibrational non-equilibrium gas flows", *International Journal of Numerical Methods in Fluids*, Vol. 14, pp. 935-60.

Anderson, J. Jr (1990a), *Hypersonic and High Temperature Gas Dynamics,* McGraw-Hill, New York, NY.

Anderson, J. Jr (1990b), *Modern Compressible Flow*, McGraw-Hill, New York, NY.

Argyris, J., Doltsinis, I.S., Friz, H. and Urban, J. (1991), "An exploration of chemically reacting viscous hypersonic flow", *Computer Methods in Applied Mechanics and Engineering*, Vol. 89, pp. 85-128.

Ben-Dor, G. and Glass, I.I. (1979), "Domains and boundary on non-stationary oblique shock-wave reflexions. 1. Diatomic gas", *Journal of Fluid Mechanics,* Vol. 92, pp. 459-96.

Ben-Dor, G. and Glass, I.I. (1980), "Domains and boundary on non-stationary oblique shock-wave reflexions. 2. Monatomic gas", *Journal of Fluid Mechanics,* Vol. 96, pp. 735-56.

Bertolazzi, E. (1995), *Risoluzione Numerica di Flussi Ipersonici Chimicamente Reattivi,* PhD thesis, Trento University, Italy.

Bertolazzi, E. (1996), "Positive and conservative schemes for mass action kinetics", *Computers and Mathematics with Applications,* Vol. 32, pp. 29-43.

Bertolazzi, E. and Casulli, V. (1993), "Fast, positive and conservative scheme for chemically reactive hypersonic flow", *International Journal of Numerical Methods for Heat & Fluid Flow,* Vol. 3, pp. 379-98.

Boris, J.P. and Book, D.L. (1973), "Flux-corrected transport", *Journal of Computational Physics,* Vol. 11, pp. 38-69.

Candler, G. (1988), "The computation of weakly ionized hypersonic flows in thermo-chemical nonequilibrium", PhD thesis, Department of Aeronautics and Astronautics, Stanford University, Stanford, CA.

Chiang, T.L. and Hoffmann, K.A., "Determination of computational timestep for chemically reacting flows", AIAA-89-1855.

Cinnella, P. and Grossman, B., "Flux-split algorithms for flows with multiple translational temperature", ICAM Report 90-06-01, Virginia Polytechnic Institute and State University, Petersburg, VA.

Colella, P. (1984), "The piecewise parabolic method (PPM) for gas-dynamical simulation", *Journal of Computational Physics,* Vol. 54, pp. 174-201.

Colella, P. and Glaz, H.M. (1985), "Efficient solution algorithms for the riemann problem for real gases", *Journal of Computational Physics*, Vol. 59, pp. 264-89.

Collatz, L. (1960), *The Numerical Treatment of Differential Equations*, Springer, Berlin.

Deschambault, R.L. and Glass, I.I. (1983), "An update on non-stationary oblique shock-wave reflections: actual isopicnics and numerical experiments", *Journal of Fluid Mechanics,* Vol. 131, pp. 27-57.

Dunn, M.G. and Kang, S.W. (1973), "Theoretical and experimental studies of reentry plasmas", NASA CR2232.

Edwards, J.R. and McRae, D.S. (1993), "Nonlinear relaxation/quasi-Newton algorithm for the compressible Navier-Stokes equation", *AIAA Journal,* Vol. 31.

Glaz, H.M., Colella, P., Glass, I.I. and Deschambault, R.L. (1985), "A numerical study of oblique shock-wave reflections with experimental comparisons", *Proc. of the Royal Society of London,* Vol. 398, pp. 117-40.

Grossman, B. and Cinnella, P. (1988), "The computation of non-equilibrium, chemically-reacting flows", *Computers and Structures*, Vol. 30, Pergamon Press, Oxford, pp. 79-93.

Groth, C.P.T. and Gottlieb, J.J. (1993), "VD finite-difference methods for computing high-speed thermal and chemical non-equilibrium flows with strong shocks", *International Journal of Numerical Methods for Heat & Fluid Flow*, Vol. 3, pp. 483-516.

Groth, C.P.T., Gottlieb, J.J. and Sullivan, P.A. (1991), "Numerical investigation of high-temperature effects in the UTIAS-RPI hypersonic impulse tunnel", *Canadian Journal of Physics,* Vol. 69, pp. 897-918.

Harten, A. (1977), "The artificial compression method for computation of shocks and contact discontinuities, I single conservation laws", *Communications on Pure and Applied Mathematics*, Vol. XXX, pp. 611-38.

Harten, A. (1983), "High resolution schemes for hyperbolic conservation laws", *Journal of Computational Physics,* Vol. 49, pp. 357-93.

Harten, A. (1984), "On a class of high resolution total-variation-stable finite-difference schemes", *SIAM Journal of Numerical Analysis*, Vol. 21, pp. 1-23.

Harten, A. (1987), "Uniformly high order accurate essentially non-oscillatory schemes, III", *Journal of Computational Physics,* Vol. 71, pp. 231-303.

Harten, A., Hyman, J.M. and Lax, P.D. (1976), "On finite-difference approximation and entropy conditions for shocks", *Communications on Pure and Applied Mathematics,* Vol. XXIX, pp. 297-322.

Häuser, J., Vinckier, A., Zemsch, S. and Paap, H.G. (1989), "Supercomputing in hypersonic flow with non-equilibrium effects", *Supercomputing in Fluid Flow,* Lowell, MA, pp. 3-5.

Hirsch, C. (1991), *Numerical Computations Of Internal And External Flows,* Wiley & Sons, New York, NY.

Hornung, H.G. (1972), "Non-equilibrium dissociating nitrogen flow over spheres and circular cylinders", *Journal of Fluid Mechanics,* Vol. 53, pp. 149-76.

Hornung, H.G. (1976),"Non-equilibrium ideal-gas dissociation after a curved shock wave", *Journal of Fluid Mechanics,* Vol. 74, pp. 143-59.

Jameson, A. (1995), "Positive schemes and shock modelling for compressible flows", *International Journal of Numerical Methods in Fluids*, Vol. 20, pp. 743-76.

Jorgenson, P. and Turkel, E. (1993), "Central difference TVD schemes for time dependent and steady state problems", *Journal of Computational Physics*, pp. 297-308.

Larrouturou, B. (1954), "How to preserve mass fraction positivity when computing compressible multi-component flows", *Journal of Computational Physics*, Vol. 95, pp. 59-84.

Lax, P.D. (1954), "Wak solutions of nonlinear hyperbolic equations and their numerical computations", *CPAM*, Vol. 7, pp. 159-93.

Lee, J.-H. (1984), "Basic governing equation for the flight regimes of aeroassisted orbital transfer vehicles", AIAA-84-1729, Snowmass, CO, June, pp. 25-8.

LeVeque, R.J. (1990), *Numerical Methods for Conservation Laws,* Birkhäuser Verlag, Berlin.

Majda, A. and Osher, S. (1979), "Numerical viscosity and the entropy condition", *Communications on Pure and Applied Mathematics,* Vol. XXXII, pp. 797-838.

Millikan, R.C. and White, D.R. (1963), "Systematics of vibrational relaxation", *The Journal of Chemical Physics,* Vol. 39, pp. 3209-12.

Ortega, J. M. (1988), "Efficient implementation of certain iterative methods", *SIAM Journal on Scientific and Statistical Computing,* Vol. 9.

Osher, S. (1984), "Riemann solvers, the entropy condition, and difference approximations", *SIAM Journal on Scientific and Statistical Computing,* Vol. 21, pp. 217-35.

Osher, S. and Chakravarthy, S. (1984), "High resolution schemes and the entropy conditions", *SIAM Journal on Scientific and Statistical Computing*, Vol. 21, pp. 955-84.

Park, C. (1984), "Problems of rate chemistry in the flight regimes of aeroassisted orbital transfer vehicles", AIAA-84-1730, AIAA, Snowmass, CO, 25-28 June.

Park, C. (1985), "On convergence of computation of chemically reacting flows" AIAA-85-0247.

Park, C. (1990), *Nonequilibrium Hypersonic Aerothermodynamics,* John Wiley & Son, New York, NY.

Rider, W.J. (1993), "Methods for extending high-resolution schemes to non-linear system of hyperbolic conservation laws", *International Journal of Numerical Methods in Fluids,* Vol. 17, pp. 861-85.

Roe, P.L. (1981), "Approximate Riemann solvers, parameter vectors, and difference schemes", *Journal of Computational Physics*, Vol. 43, pp. 357-72.

Rose, M.E. (1983), "Compact finite difference schemes for the Euler and Navier-Stokes equations", *Journal of Computational Physics*, Vol. 49, pp. 420-42.

Saltzman, J. (1994), "An unsplit 3D upwind methods for hyperbolic conservation laws", *Journal of Computational Physics,* Vol. 115, pp. 153-68.

Schröder, W. and Hartman, G. (1992), "Implicit solution of three-dimensional viscous hypersonic flows", *Computers and Fluids,* Vol. 21, pp. 109-32.

Shu, C.-W. (1987), "TVB uniformly high-order schemes for conservation laws", *Mathematics of Computation,* Vol. 49, pp. 105-21.

Shuen, S. and Yoon, S. (1989), "Numerical study of chemically reacting flows using lower-upper symmetric successive overrelaxation scheme", *AAIA Journal,* Vol. 27.

Shuen, J.S., Liou, M.S. and Van Leer, B. (1990), "Inviscid flux-splitting algorithms for real gases with non-equilibrium chemistry", *Journal of Computational Physics*, Vol. 90, pp. 371-95.

Sod, G.A. (1978), "A survey of several finite difference methods for systems of nonlinear hyperbolic conservation laws", *Journal of Computational Physics*, Vol. 27, pp. 1-31.

Steger, J.L. and Warming, R.F. (1981), "Flux vector splitting of the inviscid gas dynamic equations with application to finite-difference methods", *Journal of Computational Physics*, Vol. 40, pp. 263-93.

Swanson, R.C. and Turkel, E. (1992), "On central-difference and upwind schemes", *Journal of Computational Physics,* Vol. 101, pp. 292-306.

Sweby, P.K. (1984), "High resolution schemes using flux limiters for hyperbolic conservation laws", *SIAM Journal of Numerical Analysis*, Vol. 21, pp. 995-1011.

Tadmor, E. (1984), "Numerical viscosity and the entropy condition for conservative difference schemes", *Mathematics of Computation,* Vol. 41, pp. 369-81.

Tadmor, E. (1987), "The numerical viscosity of entropy stable schemes for systems of conservation laws. I", *Mathematics of Computation*, Vol. 49, pp. 91-103.

Toon, S. and Kwak, D. (1992), "Implicit Navier-Stokes solver for three-dimensional compressible flows", *AIAA Journal,* Vol. 30.

Van Leer, B. (1979), "Toward the ultimate conservative difference scheme", *Journal of Computational Physics,* Vol. 32, pp. 101-36.

Vincenti, W.G. and Kruger, C.H. Jr (1967), *Introduction to Physical Gas Dynamics*, Krieger Publishing Company, Malabar, FL.

Vinckier, A. (1990), "Qoneq, A first step towards 2d nonequilibrium flow", Institut für Luftfahrttechnik und Leichtbau, Universiät der Bundeswehr, München.

Vol'pert, A.I. and Hudjaev, S.I. (1985), *Analysis In Classes of Discontinuous Functions and Equations of Mathematical Physics*, Martinus Nijoff Publishers, Dordrecht.

Walpot, L. (1991), "Quasi one dimensional inviscid nozzle flow in vibrational and chemical non-equilibrium", T.U.DELFT Department of Aerospace Engineering High Speed Aerodynamics Kluyverweg 2 2629, WL Delft, The Netherlands.

Williams, F.A. (1985), *Combustion Theory 2nd Ed.*, Benjamin/Cummings Pub., Menlo Park, CA.

Witte, D.W., Tatum, K.E. and Willias, S.B. (1996), "Computation of thermally perfect compressible flow properties", AIAA-96-0681, December.

Wüthrich, S. and Sawley, M.L. (1992), "Coupled Euler/boundary-layer methods for non-equilibrium, chemically reacting hypersonic flows", *AIAA Journal,* Vol. 30, December, pp. 2836-44.

Yu, S.T., McBridge, B.J., Hsiesh, K.C. and Shuen, J.S. (1988), "Numerical simulation of hypersonic inlet flows with equilibrium or finite rate chemistry", AIAA-88-0273.

Zeidler, E. (1986), *Nonlinear Functional Analysis and its Applications I,* Springer-Verlag, New York, NY.